Astron. Astrophys. 333, 343–361 (1998)

ASTRONOMY AND ASTROPHYSICS

Gravity wave excitation and momentum transport in the solar interior: implications for a residual circulation and lithium depletion

David C. Fritts[1,⋆], **Sharon L. Vadas**[1], **and Øyvind Andreassen**[2]

[1] NWRA/Colorado Research Associates, 3380 Mitchell Lane, Boulder, CO 80301, USA
[2] Forsvarets Forskningsinstitutt, P.O. Box 25, N-2007, Kjeller, Norway

Received 20 November 1996 / Accepted 22 December 1997

Abstract. We present a conceptual model for the excitation, filtering, and anisotropic propagation of gravity waves in the stratified solar interior at and below the base of the convection zone. Excitation occurs via penetrative convection into the stratified and sheared interior, where gravity waves (or g-modes) are excited on spatial and temporal scales imposed by convection and the zonal shearing due to differential rotation. The resulting wave spectrum propagates into the solar interior with increasing anisotropy in the horizontal azimuth of propagation with increasing depth. This is due both to the preferential excitation of waves propagating against the mean flow in shear and to the filtering of the spectrum by the mean shear below the source depth. Anisotropic propagation into the solar interior induces momentum transports and accompanying body forces where the waves undergo dissipation. Because the radial shear of the zonal motion reverses sign at $\sim 37^o$, these momentum fluxes and their associated body forces are prograde at lower latitudes and retrograde at high latitudes with respect to the nearly solid-body rotation of the core. The implications of this forcing in the absence of thermal diffusion on the large scale motions are an induced residual circulation providing Coriolis torques that balance the body forces and a systematic overturning at outer radii of the solar radiative interior. For plausible estimates of the relevant spatial scales and magnitudes of gravity wave forcing, we find that the induced circulation penetrates to depths at which Lithium is destroyed and occurs on time scales that are consistent with its observed depletion and the age of the Sun. Using the same estimates, we also find that these processes cannot contribute significantly to Beryllium depletion on the same time scales.

Key words: convection – hydrodynamics – Sun: abundances – Sun: interior – Sun: oscillations – Sun: rotation

1. Introduction

Internal gravity waves, or g-modes in solar terminology, have been studied extensively in the last few decades because of their apparent or potential roles in various gravitationally stratified fluids. In the terrestrial context, such motions are now known to have far more significant influences than believed initially for several reasons. First, internal gravity waves[1] are excited in the atmosphere and oceans in many ways and are ubiquitous features of the motion spectra. The more important atmospheric sources include topography, convection, and wind shear. Oceanic sources include surface forcing and currents over bottom topography. In each case, the continuous actions of the various sources, together with the interactions among different wavefield components, contribute to wavenumber and frequency spectra spanning several decades. More importantly, however, gravity wave motions also induce significant fluxes of energy and momentum between regions of excitation and dissipation. Wave-mean flow interactions accompany wave dissipation, leading to filtering and preferential propagation in regions of shear flow and to body forces where wave momentum fluxes are divergent. These body forces are now understood to lead to induced residual circulations in the terrestrial atmosphere which contribute systematic overturning of the fluid and which may extend over considerable depths (McIntyre 1989; Garcia & Boville 1994; Fritts & Luo 1995).

In the solar context, gravity waves are expected to be present in the stably-stratified interior. Press (1981) first suggested that gravity waves would be generated by convective overshooting below the convection zone, would propagate inward and amplify geometrically near the solar core, and would lead to instability and radial mixing. Other studies have assessed the potential for gravity waves to account for the observed Lithium depletion via enhanced mixing of the outer radiative interior and for the uniformity of angular frequency with radius in the radiative interior through angular momentum transports (Press & Rybicki 1981; Knobloch 1991; Schatzman 1993, and references therein).

Send offprint requests to: David C. Fritts

⋆ This research was performed while the lead author was a Visiting Professor at the Radio Atmospheric Science Center of Kyoto University, Kyoto, Japan.

[1] Hereafter, we refer to internal gravity waves as simply "gravity waves"; "internal" refers to those motions having vertically-propagating rather than evanescent behavior.

Recent sensitive measurements of the solar wind also have been used to infer the presence of interior gravity waves (Thompson et al. 1995; see Pallé 1991, for a review), though other theories may better explain the observed spectrum (Kumar et al. 1996).

We know from simulations of solar penetrative convection and from equivalent dynamics in the terrestrial atmosphere that such convection will excite gravity waves in the solar interior. However, there is considerable uncertainty at present over the spatial and temporal scales of such convection and of the gravity waves that are excited via this process. Earlier numerical studies of solar penetrative convection have demonstrated the excitation of gravity waves on various spatial scales (Hurlburt et al. 1986, 1994). These and analytic arguments by Zahn (1991), Schmitt et al. (1984), and others suggested that convective penetration should be significant, extending as much as a pressure scale height into the stratified interior. More recent studies suggest, on the other hand, a number of mechanisms that may act to limit the efficiency of such penetration. These include instabilities which disrupt the coherence of descending plumes (Rast 1997) and rotation which organizes convection on smaller spatial scales (Julien et al. 1996a, 1996b). Shallower plume penetrations are also anticipated by other numerical simulations and helioseismological inferences (Basu et al. 1994; Gough et al. 1996; Andersen 1996). Existing simulations are further limited in their applicability to the solar interior by having neglected, to date, the effects of shear at the convective/stratified interface. Importantly, new missions and techniques for local helioseismological inversions may help to clarify these issues.

Previous efforts to address Lithium depletion via dynamical processes following the main sequence evolution have addressed possible direct mixing by penetrative convection, gravity wave instability processes, and anisotropic turbulence and advection due to differential rotation. Convective plumes penetrating significantly into the radiative interior offered an attractive mechanism for mixing to the depth at which Lithium burns (Schmitt et al. 1984; Zahn 1991). Substantially smaller penetrations, however, cannot themselves induce mixing to the required depth. Gravity waves likewise were proposed to lead to enhanced mixing of the outer radiative interior via wave instability or transport processes, thus accounting for Lithium depletion relative to elements that burn at greater depths (Press 1981; Press & Rybicki 1981; Foukal 1990; Knobloch 1991). But it has proven difficult with the proposed wave scales and penetration depths to account for the level of mixing necessary to achieve the $\sim 99\%$ Lithium depletions observed. Shear instabilities have been suggested to contribute to radial mixing by Guzik & Deupree (1996), but also appear unable to contribute significantly to Lithium depletion. Finally, anisotropic turbulence and advection arising in the shear due to differential rotation (the solar tachocline) were considered by Chaboyer & Zahn (1992), Zahn (1992), and Schatzman (1993), but appear not to contribute sufficient transport to account for Lithium depletion. The mechanism proposed by Schatzman (1993) predicts increasing mixing efficiency with increasing rotation, and is thus the wrong dependence to account for the enhanced Lithium abundances observed in stars having the highest rotation rates (Butler et al. 1987; Rebolo & Beckman 1988; Balachandran et al. 1988; García López et al. 1991; Soderblom et al. 1993). The mechanism by Zahn (1992) does predict that young, fast rotators should have higher lithium abundances, as observed. However, the theory also predicts that the Sun should have a rapidly rotating core; this is increasingly suspect because Charbonneau et al. (1997) find that the Sun's interior rotates as a solid body down to $r/R_\odot \simeq 0.1$, where $R_\odot$ is the solar radius. And recent stellar models which include diffusion and rotational mixing are able to account for the lithium depletion observed (Chaboyer et al. 1995), but only at the expense of having a large solar inner angular velocity. Because the Sun's rigid rotation occurs to a much greater depth than where the mean molecular weight gradients build up, these models are also increasingly suspect.

Main sequence events likewise appear unable to account for observed Lithium depletions or its variation with stellar rotation rate. Main sequence mass loss has been considered as a mechanism for Lithium depletion in the Hyades G-dwarfs by Swenson & Faulkner (1991, 1992), who concluded that "mass-loss cannot be a significant contributor to the depletion pattern seen in these stars". A similar conclusion was reached for the Sun by Guzik & Cox (1995). Stellar evolution models in which the convection zone and the radiative interior are dynamically isolated and in which Lithium burning occurs only within the convection zone are apparently able to account for Lithium depletions in young main sequence stars having slow rotation. However, rapidly rotating young main sequence stars exhibit little or no Lithium depletion, and hence represent a significant departure from the predictions of such models. Lithium depletion in the Pleiades was believed initially to be a purely evolutionary effect (Butler et al. 1987; Rebolo & Beckman 1988; Balachandran et al. 1988; García López et al. 1991). But Soderblom et al. (1993) have argued that the variation in Lithium abundances seen in the Pleiades is real and is a result of both stellar physics and evolution. They found that for G and K dwarfs, the variation in Lithium abundances is correlated with both rotation and chromospheric activity. From this they concluded that the connection between excess Lithium and rapid rotation is likely physical and that rapid rotation somehow enables a star to preserve more of its initial Li than a more slowly rotating star of the same mass. Thus, resolution of the Lithium depletion problem may require processes or effects not yet considered in the evolution of stellar interiors.

There are several aspects of gravity wave excitation, propagation, and dissipation which are known to have significant influences in the terrestrial atmosphere, but the implications of which appear not to have been considered at and below the convective/stratified interface of the Sun. These include

1) the effects of environmental shear on the excitation and preferential propagation and dissipation of gravity waves entering the solar radiative interior and
2) the wave-induced circulation accompanying gravity wave momentum transports and dissipation within the radiative interior.

It is our goal here to include these effects and assess their potential to account for the preferential depletion of Lithium relative to other elements. The presence of shears due to differential rotation which span the convective/stratified interface at equatorial and high latitudes (Goode et al. 1991; Tomczyk et al. 1995; Thompson et al. 1996; Charbonneau et al. 1997) are expected to have two effects. The effects include the excitation of gravity waves having a preferred direction of propagation and a filtering of incident wave motions so as to suppress vertical propagation for one azimuth of propagation and enhance it for the opposite. In this way, gravity waves having both a preferred direction of propagation and larger amplitudes, vertical wavelengths, and group velocities (hence greater penetration depths) are able to influence the solar interior.

A second aspect of gravity wave propagation and mean-flow interaction not yet considered in the solar (or stellar) context is the wave-induced residual circulation accompanying wave momentum transports and momentum flux divergence due to wave dissipation. Yet we know from terrestrial analogs that the mechanisms required for such gravity wave forcing and responses are virtually certain to be operative in the outer radiative interior of the Sun, barring significant thermal diffusion damping of these induced large-scale motions. For example, the gravity wave induced circulation near the terrestrial mesopause under solstice conditions is sufficiently strong to drive the atmosphere far from radiative equilibrium (Garcia 1989; McIntyre 1989; Fritts & Luo 1995). Specifically, we believe that the inclusion of shear influences on wave excitation and propagation and the induced residual circulation accompanying wave dissipation at greater depths provides a plausible scenario by which gravity waves can account for the observed Lithium depletion within the age of the Sun. Such gravity wave effects will occur at those radii at which there are the greatest uncertainties in the physics of the standard solar models (SSM); they also likely represent minute departures from SSM solar structure predictions well within the small discrepancies relative to current helioseismological inferences (Christensen–Dalsgaard et al. 1996).

Our goal in this paper is to demonstrate that the combined effects of the solar tachocline on gravity wave excitation and propagation and the residual circulation arising from wave momentum transports and dissipation provide a plausible, viable mechanism for solar Lithium depletion. This depletion would occur via overturning of the outer radiative interior on time scales consistent with $\sim 99\%$ Lithium depletion within the solar age, while implying very little Beryllium depletion on the same time scales. Because the magnitude of the residual circulation is inversely proportional to the rotation rate, this model also may account for the enhanced Lithium abundances observed in stars exhibiting faster rotation. Thermal diffusion effects on the large-scale induced motion are neglected here in order to solve for the residual circulation analytically. These effects are being included, however, in a numerical modeling effort at present. The important issues are the temporal and spatial scales of the relevant gravity waves, the momentum flux profiles that accompany penetrative convection and shear below the convective/stratified interface, and the distribution of the induced residual circulation with depth in response to wave dissipation. While solar gravity wave parameters can only be guessed at this stage, we note that there are a range of possible wave parameters that could provide the relevant forcing and effects. More precise assessments of such wave effects will await further definition of solar wave scales via additional modeling or observational studies.

This paper is organized in the following manner. We first discuss in Sect. 2 the characteristics, dissipation scales, and azimuthal dependence of waves propagating into the stratified solar interior. In Sect. 3 we describe the mechanisms we believe contribute primarily to excitation and preferential zonal propagation of gravity waves and to their spatial and temporal scales. Sect. 4 examines the implications of these sources and gravity wave scales for wave filtering and momentum fluxes. The manner by which gravity waves force a residual circulation and an estimate of the strength and character of this circulation are addressed in Sect. 5. Sect. 6 considers the implications for the depletion of Lithium and Beryllium. A summary and our conclusions are provided in Sect. 7.

2. Gravity wave propagation and dissipation in shear

We begin our analysis of possible gravity wave forcing of the solar interior by considering the implications of differential rotation and dissipation for the penetration of gravity waves having various spatial and temporal scales and azimuths of propagation. For present purposes, we are concerned with the effects of shear at the convective/stratified interface rather than with the processes which may act to maintain this shear, which is itself an open question (Thompson et al. 1996). Thus, we will assume for now that the tachocline shear is externally applied, though in reality the processes we describe may contribute to its maintenance or evolution below the convective/stratified interface. We will consider primarily waves having spatial scales very much smaller than the solar radius. More importantly, we will focus on waves in a tachocline that is deep compared to characteristic gravity wave scales and which may, depending on the azimuth of wave propagation, lead to strong wave-mean flow interactions. Under these conditions, a modal description of gravity wave propagation in the solar interior cannot account for all of the possible motions or influences. This is because such an approach excludes motions having phase velocities equal to the mean fluid velocity at some depth. Thus we adopt a local wave, rather than a global, modal description of wave propagation, dissipation, and interactions. [2] We will also refer to the relevant motions as gravity waves rather than g-modes to make this distinction explicit.

2.1. Gravity wave notation and structure

Because much of our subsequent discussion concerning the effects of stratification and shear on gravity wave propagation might be new to readers, we will provide here a definition and discussion of terms that will be used in our development. We use

[2] We will nevertheless use a global approach to solve the mean-flow equations in Sect. 5.

$\mathbf{k}_{tot} = (\mathbf{k}, m)$ to denote the wavenumber vector, with horizontal and vertical components $\mathbf{k}$ and m, and associated horizontal and vertical wavelengths $\lambda_h = 2\pi/k$ and $\lambda_z = 2\pi/m$, respectively, where $k = |\mathbf{k}|$ and vertical is defined as in the direction of gravity, $-\mathbf{g}$. Then a gravity wave propagating with horizontal phase speed c greater than the component of the mean flow speed $\overline{u}_c$ in the horizontal azimuth of propagation will have a frequency $\omega = kc > 0$, an intrinsic horizontal phase speed $c_i = c - \overline{u}_c$, and an intrinsic frequency $\omega_i = k(c - \overline{u}_c)$. Note that the phase velocity is in the horizontal direction of propagation, $\mathbf{c} = c\mathbf{k}/k$, and that k, $c = |\mathbf{c}|$, and c_i are defined to be positive. As we will demonstrate below, it will be sufficient to consider wave motions that have intrinsic frequencies $\omega_i \gg f$ and vertical wavelengths $\lambda_z \ll H$, where $f = 2\Omega \sin\phi$ is the inertial frequency (or Coriolis parameter), Ω is the local solar rotation frequency, ϕ is latitude, $H = -(1/\overline{\rho})d\overline{\rho}/dr$ is the local density scale height, and T is temperature.

Motivated by the thin geometry appropriate for this problem, we employ the following Cartesian geometry at the location of interest at the convective/stratified interface. We fix the orientation of the reference frame for any latitude ϕ with x in the zonal (prograde) direction, y in the meridional direction, and z in the outward, radial direction. In addition, θ defines the horizontal azimuth of wave propagation measured clockwise from the $+x$ axis relative to the mean fluid motion at that depth. Thus, a wave propagates in the prograde direction with respect to the mean fluid motion (with a component of the intrinsic phase speed toward positive x) if $-\pi/2 < \theta < \pi/2$, and in the retrograde direction (toward negative x) if $\pi/2 < \theta < 3\pi/2$. Fig. 1 a and b show the orientation of this coordinate system at latitude ϕ with respect to the Sun.

Now assume that a wave has velocity perturbations of the form $e^{i(\mathbf{k}\cdot\mathbf{x}_h + mz - \omega t)} e^{z/2H}$, where $\mathbf{x}_h = x\mathbf{i} + y\mathbf{j}$ is the distance vector in the horizontal plane, and m is slowly varying with depth. We also assume that k and c do not change as the wave propagates into the stratified interior, though this is not strictly true in a spherical fluid or in the presence of wave-mean flow interactions. Then the linear, inviscid equations of motion for a sheared and stratified fluid, neglecting curvature of the mean shear flow, $d^2\overline{u}/dz^2$, yield a dispersion relation of the form (Gossard & Hooke 1975)

$$m^2 = \frac{k^2 N^2}{\omega_i^2} - k^2 = \frac{N^2}{(c - \overline{u}_c)^2} - k^2, \qquad (1)$$

where N is the local buoyancy (or Brunt-Väisälä) frequency, assumed to be constant here. This is a good approximation sufficiently below the convective/stratified interface since the density scale height is then nearly constant with depth (Zirin 1988, page 101). The exponential factor in the assumed wave form is implied by the exponential decay of density with height (or radius). For convenience, we take the reference frame in which c and $\overline{u}_c$ are specified to be fixed at the depth of the convective/stratified interface ($z = 0$). In this reference frame, $\overline{u}$ is the mean motion toward positive x ($\theta = 0$) and mean motions in the y and z directions are assumed negligible for purposes of wave propagation. In addition,

$$\overline{u}_c = Sz\cos\theta \qquad (2)$$

is the projection of the mean motion in the azimuth of horizontal wave propagation θ, and $S = d\overline{u}/dz$ is the vertical shear of the mean zonal motion.

A gravity wave propagating downward into the solar interior with azimuthal propagation direction θ will have horizontal (azimuthal) and vertical perturbation velocities u'_w and w'_w, respectively. These are related through the approximate continuity equation for such two-dimensional motions, $\boldsymbol{\nabla}\cdot\boldsymbol{v} = 0$, such that $ku'_w \simeq -mw'_w$. For a wave motion with prograde and downward propagation, we expect $u'_w w'_w < 0$. This implies that $m > 0$ because $k > 0$. Wave motions for which $m^2 \gg k^2$ are referred to as hydrostatic, in which case vertical accelerations are small and the vertical momentum equation represents an approximate balance between gravitational and pressure gradient terms. The horizontal and vertical components of the group velocity for such a motion are $c_{gh} = \partial\omega_i/\partial k$ and $c_{gz} = \partial\omega_i/\partial m$, respectively. With the above definitions and assumptions, $\omega_i \simeq kN/m > 0$ and the horizontal and vertical components of group velocities in the frame of reference of the mean flow are $c_{gh} = N/m = \omega_i/k > 0$ and $c_{gz} = -\omega_i/m < 0$. The corresponding components of phase velocity, ω/k and ω/m, are aligned and anti-aligned, respectively, with the group velocity components, such that upward phase progression in the frame of the mean horizontal motion corresponds to downward wave propagation.

2.2. Propagation and dissipation in the solar interior

Recent solar experiments (Tomczyk et al. 1995; Thompson et al. 1996; Charbonneau et al. 1997) have found that nearly all of the middle to outer radiative interior of the Sun rotates as a solid body. Distinctly below the convection zone (at $r \simeq (0.66 \pm .02)R_\odot$) however, the angular frequency begins to vary at an approximately constant rate with radius out to a radius of $r \sim 0.8$ $R_\odot$. This variation of angular frequency with radius is latitude dependent, however, with increasing angular frequency with increasing radius at latitudes up to $\phi \sim 37^o$ and decreasing angular frequency with increasing radius at higher latitudes. In our chosen reference frame, then, solar differential rotation implies negative (retrograde) mean zonal velocities at equatorial latitudes and positive (prograde) mean zonal velocities at higher latitudes below the convective/stratified interface.

We now assume that wave excitation occurs predominantly at and below the convective/stratified interface at $r \simeq (0.713 \pm 0.003)R_\odot$ (Christensen–Dalsgaard et al. 1991). To calculate the radial shear of the zonal velocity, we compute the difference between the inferred helioseismic velocity profile and the velocity profile that would be present if the convective and radiative regions rotated as a solid body. Over the range of radii from 0.66 to 0.713 $R_\odot$, this yields a velocity difference of $\sim$ 40 to 60 m s^{-1} at equatorial latitudes and $\sim$ 40 m s^{-1} with the opposite sign at $\phi \sim 60^o$.

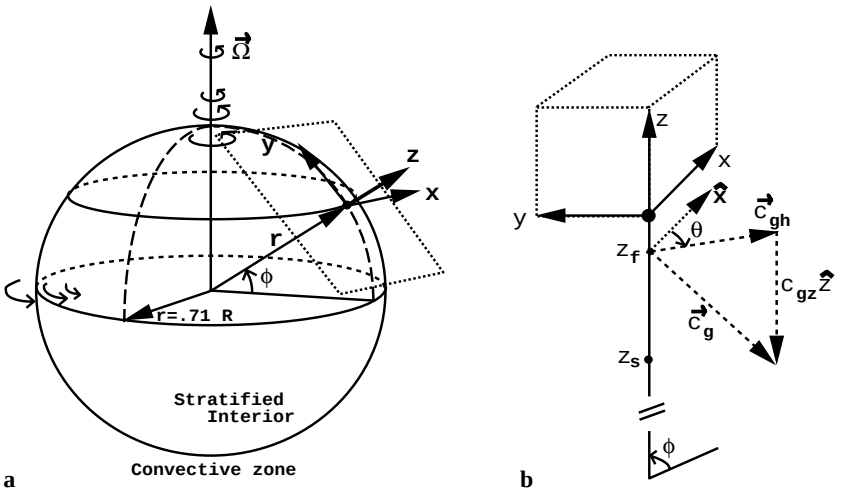

Fig. 1. a Schematic showing the orientation of the Cartesian coordinate system at latitude ϕ. The coordinate system is oriented tangential to the convective/stratified interface at $r \simeq 0.713 R_\odot$, with the z axis in the radial direction, the x axis in the zonal direction, and the y axis in the meridional direction. Also shown schematically is how the angular velocity increases (decreases) with radius at the equator (pole) with increasing radius. **b** Schematic of the notation and direction of wave propagation below the convection zone. The shear ends at $z = z_s$, waves are assumed to be excited at $z = z_f$, the group velocity $\mathbf{c}_g = (\mathbf{c}_{gh}, c_{gz})$ is downward and in the direction of horizontal wave propagation with respect to the mean zonal motion, and the horizontal component of phase velocity, $\mathbf{c}_{gh}$, is at an angle θ measured clockwise from the x axis relative to the mean zonal motion.

As will be demonstrated below, we expect gravity waves to be excited with horizontal phase speeds centered about $\mathbf{c} = 0$ at the depth to which convective plumes penetrate, $z = z_f < 0$, with magnitudes $|\mathbf{c}| \sim 10$ to 100 m s^{-1} and propagation in all azimuths, θ. Given the likely nature of the forcing and the filtering effects of an environmental shear, however, we also anticipate preferred horizontal propagation in azimuths opposing the mean flow at z_f and below. Relative to the solar interior, then, such a wave spectrum will have characteristic (prograde) intrinsic phase speeds of $c_i \sim 10$ to 100 m s^{-1} or greater at equatorial latitudes, with the reverse at high latitudes.[3] For our purposes here, it will be sufficient to consider only the equatorial case and assume that high latitudes exhibit the opposite response. In both cases, it is clear from the dispersion relation, Eq. (1), that these waves will have vertical structure that is highly dependent on their azimuthal propagation, their local phase speeds, and their horizontal scales.

To illustrate the influences of gravity wave structure and mean shear on vertical wave propagation, we consider the fate of waves having different azimuths of horizontal propagation, phase speeds, and horizontal scales subject to mean shear effects and radiative diffusion. A wave with horizontal propagation at azimuth θ and initial phase speed c at $z \simeq z_f$ will experience a velocity shear as it propagates to greater depths, yielding an intrinsic phase speed given by

$$c_i = c - \overline{u}_c(z) = c - Sz\cos\theta, \tag{3}$$

with $\overline{u}_c$ and S as defined above. Here, c_i is always positive because it is defined in the intrinsic reference frame of the wave (with respect to the mean flow). For prograde propagation then, c_i increases with depth at equatorial latitudes and decreases with depth at high latitudes. The reverse dependence occurs for retrograde propagation.

[3] Hereafter, we will refer to latitudes greater than 37^o as "high latitudes".

2.2.1. Critical level filtering

Referring to Eq. (1), we note two limits having important implications for vertical propagation. One, termed a critical level, occurs where $c_i \to 0$ as the gravity wave phase speed approaches the mean fluid motion in its azimuth of propagation ($c \to \overline{u}_c$). This causes a reduction in the vertical wavelength of the wave, a slowing of its vertical propagation, and its eventual removal from the wave field via dissipation or radiative diffusion. Thus, critical levels remove wave motions having retrograde (prograde) propagation relative to the mean velocity at the source depth at equatorial (high) latitudes, provided their phase speeds are within the range of tachocline velocities at greater depths in their azimuth of horizontal propagation. The condition for which a critical level is encountered may be expressed as

$$0 \le Sz_f\cos\theta < c < Sz_s\cos\theta, \tag{4}$$

where $z_s \simeq -0.053 R_\odot \sim -H/2$ is the depth of the shear below the convective/stratified interface. Note that critical levels can only be encountered if $S\cos\theta < 0$. Propagation of waves undergoing critical level absorption then is always retrograde ($\pi/2 < \theta < 3\pi/2$) at equatorial latitudes and prograde ($-\pi/2 < \theta < \pi/2$) at high latitudes. The magnitudes of the shears and differential velocities are determined from the differential rotation data of Tomczyk et al. (1995) and yield $S \simeq 10^{-6}$ s^{-1} and $\overline{u}_s = |Sz_s| \simeq 40$ m s^{-1} at equatorial and high latitudes. [4] Critical level filtering thus imposes a preferential sense of propagation, and of momentum transport, by the surviving components of the motion field at greater depths. The cumulative effects of the various processes influencing wave penetration into the solar interior are addressed further below.

[4] The differential velocity is actually $\simeq 60$ m s^{-1} at the equator, but a steady, wave-driven circulation cannot occur without rotation and we therefore confine our attention to extra-equatorial latitudes.

2.2.2. Wave evanescence

A second limit apparent from Eq. (1) occurs when c_i varies in such a manner that $m^2 \rightarrow 0$ at some depth. In such cases, the wave character changes from being vertically propagating where $m^2 > 0$ to vertically evanescent where $m^2 < 0$, with evanescent structure implying an exponential decay of wave amplitude with depth. This behavior results in the reflection of the wave and its trapping within the region with $m^2 > 0$. Such evanescent structure can occur for waves having either prograde or retrograde propagation. We also note that evanescent structure and the amplitude attenuation that results does not exclude waves from the solar interior entirely.

Consideration of shear influences near the convective/ stratified interface suggests that waves having small horizontal scales (large k) and prograde propagation (with small θ) at large initial phase speeds will be especially susceptible to such trapping. Such waves will have large intrinsic phase speeds at the source depth and will experience an increase of these intrinsic phase speeds with increasing depth (at equatorial latitudes). If these increases cause

$$c_i^2 > N^2/k^2 \tag{5}$$

within the tachocline, then $m^2 < 0$ at all greater depths and the waves will neither propagate nor transport momentum into the solar interior. Over the depth of the shear, this expression may be written for general azimuths of propagation as

$$c - Sz_s \cos\theta > N/k \tag{6}$$

or

$$k > \frac{N}{c - Sz_s \cos\theta}. \tag{7}$$

Vertically evanescent behavior can also occur for large retrograde phase speeds satisfying Eq. (5). In this case, however, the initial depth of evanescence will occur adjacent to the source depth because that is where retrograde intrinsic phase speeds are largest.

2.2.3. Radiative damping

A final effect that we consider in this section is the penetration scale for gravity waves defined in terms of the exponential damping of wave amplitudes by radiative diffusivity, κ. In the solar interior, the heat flux is carried by radiation. Using the diffusion approximation, the radiative heat flux can be written (Clayton 1983) as

$$\mathbf{q} = -\frac{4ac}{3\kappa_R \rho} T^3 \nabla T = -k \nabla T, \tag{8}$$

where $a = 8\pi^5 k_B^4/(15h^3c^3) = 7.54 \times 10^{-16}\,\mathrm{J\,m^{-3}\,K^{-4}}$, κ_R is the Rosseland mean opacity, and k is the thermal conductivity. At the bottom of the convection zone, $T \simeq 1.9 \times 10^6 K$, $\rho \simeq 160\,\mathrm{kg\,m^{-3}}$, and $\kappa_R \simeq 2.5\,\mathrm{m^2/kg}$ (Huebner 1986). The thermal diffusivity is related to k as

$$\kappa = \frac{k}{C_p \rho} = \frac{(\gamma - 1) 4acT^3}{3\gamma R \kappa_R \rho^2}. \tag{9}$$

Thus, $\kappa \approx 10^3\,\mathrm{m^2\,s^{-1}}$ at the bottom of the convection zone (Gough 1977).

The time scale for this damping for a wave with vertical wavenumber m (assuming for the present that $m^2 \gg k^2$) is $T_d \sim 1/\kappa m^2$. Then given that wave energy propagates inward at the vertical group velocity of the wave, $c_{gz} = \partial\omega_i/\partial m \simeq -\omega_i/m \simeq -\lambda_z/T_i$, where $T_i = 2\pi/\omega_i$ is the intrinsic wave period, we can define a penetration depth as $L_d \simeq -c_{gz} T_d$. This represents the depth over which a wave decreases in amplitude by e or in energy (or momentum flux per unit mass) by e^2. Expressing these quantities in terms of the wave scales using Eq. (1), we obtain

$$L_d \simeq \frac{\omega_i}{\kappa m^3} \simeq \frac{kN}{\kappa m^4} \simeq \frac{N\lambda_z^4}{8\pi^3 \kappa \lambda_h}. \tag{10}$$

For reference, this is similar to the expression obtained by Townsend (1965) and identical to that employed by Press (1981) (also see Schatzman 1993). Thus, penetration into the solar interior is strongly favored for waves having large vertical scales and small horizontal scales, though with our assumption above that $\lambda_z \ll \lambda_h$. Since the ratio of vertical to horizontal scales is given approximately by $\lambda_z/\lambda_h \simeq \omega_i/N$ and $\lambda_z \simeq 2\pi c_i/N$ for $m^2 \gg k^2$ (i.e., hydrostatic wave motions), we see also that penetration is favored for waves having high intrinsic frequencies or large intrinsic phase speeds.

2.2.4. Scale selection

The issues for gravity wave propagation and dissipation, then, are what wave scales are excited effectively by convection and shear effects at the convective/stratified interface and which of these wave scales and azimuths of propagation can survive shear effects and radiative damping and thus influence the dynamics of the solar interior. To define the constraints, we choose differential velocities of 40 and 20 m s^{-1} as representative of all but equatorial latitudes, assume strictly prograde/retrograde propagation ($\theta = 0$ and π), and note that the 20 m s^{-1} case also describes propagation in the stronger shears at azimuths of $\pm\pi/3$ and $\pm 4\pi/3$ (or at latitudes $\phi = 30^o$, 45^o, and 80^o). We further assume a buoyancy frequency $N = 1.2 \times 10^{-3}\,\mathrm{s^{-1}}$ (a buoyancy period $T_b \sim 1.5$ h) (Brown et al. 1986; Zirin 1988; Turck-Chièze et al. 1993) and consider phase speeds at the source depth as large as $100\,\mathrm{m\,s^{-1}}$ and horizontal wavelengths ranging from ~ 60 to 6000 km. The latter choices will be seen below to pose reasonable bounds on those scales expected to be excited by convection and shear at the convective/ stratified interface.

With these choices of parameters, we can use Eqs. (4), (6), and (10) to define those regions of phase speed-wavenumber space in which gravity waves

1) are excluded from penetration into the solar interior by critical levels,
2) are diminished in amplitude due to wave evanescence,
3) are attenuated by radiative diffusion, or
4) have vertical (radial) propagation that is relatively less influenced by dissipation and shear effects.

These various possibilities are summarized in semilog plots for zonal propagation ($\theta = 0$ and π) and $\overline{u}_s = 40$ and $20\,\mathrm{m\,s^{-1}}$ in the upper and lower panels of Fig. 2. The vertical axes are logarithmic and labeled by k (in $\mathrm{m^{-1}}$) and λ_h (in km) and the horizontal axes are labeled by $c * \mathrm{sign}(S\cos(\theta))$ in $\mathrm{m\,s^{-1}}$, where $\mathrm{sign}(q)$ is the sign of the quantity q. Hatched areas denote wave phase speeds excluded by critical levels for retrograde (prograde) propagation relative to the convective/stratified interface at equatorial (high) latitudes. Light and dark shaded regions at larger phase speeds and wavenumbers denote phase speed-wavenumber combinations for which waves are evanescent within part or all of the tachocline. The boundaries of these regions are labeled "f" and "s" to indicate evanescent behavior at z_f and z_s, respectively. Dashed lines labeled e^{-1} and e^{-3} denote attenuations by these factors due to radiative diffusion, with the phase speed-wavenumber combinations damped more severely than e^{-3} denoted by shading increasing with damping. Contours labeled "gw" denote our assumed gravity wave source scales and phase speeds (to be discussed further in the following section).

Several aspects of wave propagation and attenuation displayed in Fig. 2 warrant additional discussion. The most important influence is that of the tachocline. This is because shear acts, both for large and smaller differential velocities, to filter the phase speed spectrum and thus assign differential propagation and survival of waves having common initial characteristics, but opposite directions of propagation. This occurs in two ways. Critical levels remove all waves having phase speeds within the range of tachocline velocities. Radiative damping effects are also centered around the shear layer beneath z_f and thus play a larger role in the attenuation of waves that have retrograde (prograde) propagation at equatorial (high) latitudes. The combined effects of critical levels and radiative damping insure a strong anisotropy in the wave motions surviving at greater depths, with the faster prograde (retrograde) phase speeds surviving more effectively at equatorial (high) latitudes. Also seen by comparing the upper and lower panels of Fig. 2 is a tendency for even the surviving waves to be more strongly attenuated for smaller differential velocities, thus implying a "zonal focusing" of the surviving waves with increasing depth.

3. Gravity wave excitation by convection and shear

Excitation of gravity waves in a stably stratified fluid by adjacent penetrative convection has been studied in several contexts. In the solar interior, gravity wave excitation is presumed to arise in response to convective plumes penetrating the stratified solar interior. The nature and vigor of the plumes providing this forcing is uncertain at present because current models of solar convection are unable to describe the flow structure over the full depth of the convection zone. Plume penetration was initially suggested to reach a significant fraction of a scale height in semi-analytic studies by Schmitt et al. (1984) and Zahn (1991) and numerical simulations by Hurlburt et al. (1986, 1994). More recent analyses have implied stronger constraints and penetration depths of ~ 0.1 H or less (Gough et al. 1996; Julien et al. 1996a, 1996b). There is also uncertainty over the scales and velocities associated with convective plumes. The arguments by Cattaneo et al. (1991) and numerical studies by Hurlburt et al. (1986, 1994) imply intense, localized descending jets with potentially large velocities, while others suggest penetrative velocities of only $\sim 10\,\mathrm{m\,s^{-1}}$ (Rieutord & Zahn 1995; Bonin & Rieutord 1996). Thus, we must ascribe a high degree of uncertainty to the scales and energetics of the convective activity and to the possible wave structures that result. More importantly for our purposes here, however, there has been until now no attempt of which we are aware to consider the influences of shear on solar penetrative convection and the gravity wave activity that it excites. Yet it is clear in other contexts that shear may play a large role in assigning the scales and anisotropy of the resulting gravity wave motions.

Convective excitation of gravity waves is relatively better understood in the terrestrial atmosphere, where it has been the subject of numerical simulation and direct observation for many years. These efforts have identified the spatial and temporal scales of gravity waves excited by convection under a variety of flow conditions. Numerical simulations have shown boundary-layer convection to launch gravity waves which in turn act to organize the convection on larger scales of motion (Clark et al. 1986). Aircraft measurements in the vicinity of large convection have revealed these cells to excite significant wave activity having preferred azimuths of propagation (Pfister et al. 1986; Alexander & Pfister 1995), while airglow observations have demonstrated the ability of such motions to propagate over considerable depths (Taylor & Hapgood 1988). Recent modeling efforts have likewise demonstrated that convective forcing of a sheared and stratified layer leads to excitation of gravity waves having a preferred sense of propagation and momentum transport (Hauf & Clark 1989; Fovell et al. 1992; Alexander et al. 1995), analogous in many respects to flow over topography.

Modeling and observations of terrestrial gravity wave propagation, filtering, and interactions with larger scales of motion have also revealed a tendency for gravity waves to acquire a sense of horizontal propagation opposing the large-scale flow. Strong mean zonal wind structures arise in both summer and winter hemispheres under solstice conditions due to seasonal variations of the equator-to-pole thermal gradients that accompany solar heating. The strong zonal winds at greater altitudes influence the upward propagation of gravity waves and lead to the preferential propagation of waves with phase velocities aligned against the zonal flows and to gravity wave momentum fluxes that are anticorrelated with these zonal winds (Holton 1983; Vincent & Reid 1983; Fritts & Yuan 1989; Tsuda et al. 1990). Filtering by tidal wind structures likewise results in wave momentum fluxes that are anticorrelated with the tidal winds (Fritts & Vincent 1987; Fritts & VanZandt 1993; Eckermann & Marks 1996). In each case, the simplest view of this process is that the local velocity shear removes or suppresses those components of the wave spectrum experiencing a decreasing intrinsic horizontal phase speed, $c - \overline{u}_c \to 0$, while enhancing the vertical propagation of those components having the opposite sense of propagation. Because propagating gravity waves

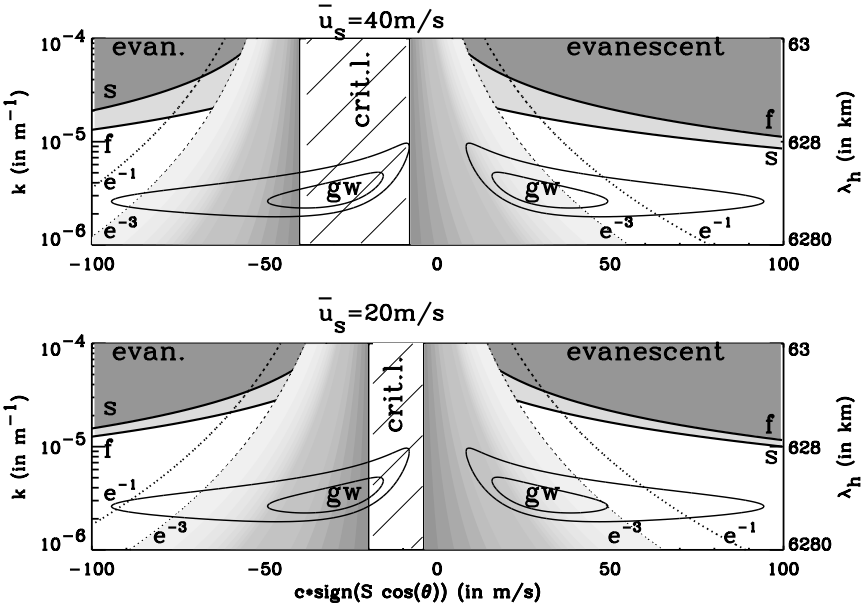

Fig. 2. The influences of a vertical (or radial) shear of the mean zonal motion on gravity wave propagation are shown for differential velocities of $\overline{u}_s = 40$ (top) and 20 (bottom) m s^{-1}. Here, positive values of $c\mathrm{sign}(S\cos\theta)$ denote prograde (retrograde) propagation with respect to the absolute reference frame (at $z = 0$, $\overline{u}_c = 0$) at equatorial (high) latitudes and negative values denote the opposite. In each case, waves having $\mathrm{sign}(S\cos\theta) < 0$ and within the range of mean zonal velocities are subject to critical level absorption (the hatched regions). Regions of wave evanescence are shaded with boundaries at z_f and z_s denoted "f" and "s", respectively; preferred gravity wave source scales are contoured and denoted "gw"; and curves of constant attenuation by factors of e^{-1} and e^{-3} are shown as dotted lines.

transport horizontal momentum in the direction of their vertical group velocity, such filtering by shear imposes an increasing anisotropy with altitude in the azimuth of horizontal propagation. The corresponding momentum flux per unit mass, $\overline{u'w'}$, summed over all spectral components, likewise achieves an increasing anisotropy with altitude, and is normally strongly anticorrelated with the mean shear flow. Here, u' and w' are the wave perturbation velocities in the azimuth of horizontal propagation and the vertical. Note that the momentum flux for an isotropic spectrum is zero because contributions from oppositely propagating components cancel.

The implications of these terrestrial results for gravity waves excited by solar penetrative convection in the presence of an environmental shear are several. First, the resulting waves must exhibit some sensitivity to the spatial and temporal scales of the plumes accounting for their generation. Perhaps more importantly for our purposes here, the excitation must favor gravity waves with a sense of propagation against, or a horizontal phase speed opposite to, the fluid motion past the convective plumes. Environmental shears at greater depths will further accentuate this tendency. This latter aspect of solar convection appears not to have been considered previously, but is central to the wave-driven influences within the solar interior that comprise the thesis described below.

We now proceed with an estimation of the likely gravity wave scales, frequencies, and intensities arising in response to penetrative convection and due to differential motion of stably stratified fluid over these convective plumes.

3.1. Excitation by penetrative convection

Based on the expectation of narrow, widely-distributed downdrafts at greater depths within the convection zone, we assume horizontal plume scales comparable to or smaller than the granulation scales of the photosphere, typically 1000 km or less. This assumption appears justified by the tendency in three-dimensional (3D) numerical simulations by Cattaneo et al. (1991) and others for downdrafts to coalesce into narrow jets which undergo horizontal contraction due to increasing density with depth. Theoretical studies also find that isolated plumes contract during descent (Arendt 1993). However, other arguments suggest that the size of the plumes may increase with depth due to turbulent entrainment (Rieutord & Zahn 1995). There are, thus, considerable uncertainties in these scales due to the range of processes likely to influence plume energetics, coherence, and stability (Julien et al. 1996a, 1996b; Rast 1997). We also assume horizontal plume velocities to be representative of the mean zonal velocity at this depth (assumed to be 0.713 $R_\odot$), though in reality it appears more likely that the descending plumes will have net prograde momentum relative to this depth due to the large-scale tachocline shear and the tendency for descending plumes to retain their horizontal velocities from shallower depths.

We can now follow any of several routes in estimating additional convective plume and gravity wave parameters. If we first take a plume downdraft velocity of $w'_p \sim 10\,\mathrm{m\,s^{-1}}$, a horizontal plume scale of ~ 1000 km, corresponding gravity wave horizontal wavelengths ~ 1000 to 3000 km, and a penetration depth $\zeta' \sim 0.1H$ as given, we can infer characteristic plume periods of $T_p \sim \zeta'/w'_p \sim 8$ days and horizontal phase speeds of $c \sim \lambda_h/T_p \sim 1$ to $3\,\mathrm{m\,s^{-1}}$.

Defining $\omega_p \simeq 2\pi/T_p$, noting that the intrinsic frequencies are of order ω_p, and assuming that $m^2 \gg k^2$, the vertical wavelengths from Eq. (1) are

$$\lambda_z \sim \omega_p \lambda_h / N. \tag{11}$$

With a buoyancy frequency of $N = 1.2 \times 10^{-3}\,\mathrm{s^{-1}}$ as before, $\lambda_z \sim 7$ to 20 km. Smaller plume penetrations with comparable velocities would yield shorter periods and larger vertical wavelengths and phase speeds. But these small expected plume velocities appear unable to couple effectively to the larger ver-

tical scales for which vertical penetration is more effective (see below).

If we assume, alternatively, that the duration of a typical convective plume is $T_p \sim 10$ to 30 hours, consistent with recent 2D and 3D models, then the characteristic wave frequencies for convectively-generated gravity waves are larger. Together with the horizontal scales assigned by the plume geometry, this implies characteristic phase speeds of $c = \omega_p/k \sim \lambda_h/T_p \sim 10$ to $30\,\mathrm{m\,s^{-1}}$ and characteristic vertical wavelengths using Eq. (1) of $\lambda_z \sim \omega_p \lambda_h/N \sim 50$ to 150 km at the source depth for $\lambda_h = 1000$ km, and three times these phase speeds and vertical wavelengths for $\lambda_h = 3000$ km. In all of these estimates, we must also remember that once excited the gravity waves will immediately begin to evolve in and be influenced by their environment, with the results being very different for differing scales and azimuths of propagation.

Gravity wave amplitudes are more difficult to assess quantitatively. However, we are able to assign upper limits to the amplitudes that can be excited at any given scale. A reasonable upper limit for forced wave amplitudes is the constraint imposed by convective or shear instability within the local wave field. In terrestrial applications with a Prandtl number Pr ~ 1, it is typically the convective instability that poses the limit for waves having intrinsic frequencies $\omega_i^2 \gg f^2$ (Fritts 1984b; Andreassen et al. 1994; Fritts et al. 1994; Winters & D'Asaro 1994). However, when damping occurs primarily by radiative diffusion, we might expect local convection to be inhibited and to experience amplitude limits imposed instead by shear instability. In either case, the relevant constraint is approximately

$$u'_w \sim c_i = c - \overline{u}_c, \tag{12}$$

where u'_w is the horizontal velocity perturbation of the gravity wave in the azimuth of propagation and the subscript w denotes a wave quantity. It is also very difficult to force a wave, even with a quasi-monochromatic source, at an amplitude approaching the saturation limit imposed by Eq. (12). A more defensible limit might be $u'_w \sim \alpha c_i$ with $\alpha \sim 0.5$ or less and suggests, with the above estimates of phase speeds, gravity wave amplitudes of

$$u'_w \sim 5 - 15\,\mathrm{m\,s^{-1}} \tag{13}$$

for $\lambda_h = 1000$ km, and three times these values for $\lambda_h = 3000$ km.

Alternatively, we can relate the vertical kinetic energy flux of the wave field to that of the convective plume, assuming that a fraction β of the kinetic energy of the descending plume having a time scale T_p can be communicated effectively to the gravity wave field in the solar radiative interior. Thus, we obtain

$$\frac{1}{2}\beta {w'_p}^3 \sim \frac{1}{2} c_{gz} {u'_w}^2, \tag{14}$$

where $c_{gz} \simeq \lambda_z/T_p$ is the vertical group velocity of the gravity waves excited by penetrative convection and we have assumed approximately hydrostatic wave motions for which the horizontal velocity is the major contributor to the kinetic energy. In general, c_{gz} exhibits considerable uncertainty because it varies quadratically with λ_z for fixed λ_h. For the parameters discussed, with $\beta \sim 0.5$ and $c_{gz} \sim 0.5$ to $5\,\mathrm{m\,s^{-1}}$ for $\lambda_h = 1000$ km and $c_{gz} \sim 1.5$ to $15\,\mathrm{m\,s^{-1}}$ for $\lambda_h = 3000$ km, we obtain estimates of $u'_w \sim 3$ to $10\,\mathrm{m\,s^{-1}}$ and $u'_w \sim 10$ to $30\,\mathrm{m\,s^{-1}}$ for the two assumed horizontal wavelengths, respectively. These are generally consistent with the estimates based on saturation constraints obtained above.

Given these estimates of horizontal wave velocities and the wave periods assumed to be imposed by convective forcing, we can now estimate the corresponding vertical velocities and the vertical fluxes of horizontal momentum by these waves into the solar interior. Of the convectively-imposed periods discussed above, those that seem most plausible for the deeper plumes, given the degree of stratification of the solar interior, are $T_p \sim 10$ to 30 hours. The estimate $T_p \sim 8$ days seems appropriate only for the more weakly stratified fluid near the convective/stratified interface and thus may apply only to very shallow plume penetrations. Assuming now that the shear due to differential rotation plays no role in assigning the intrinsic properties of the excited waves and that these motions are initially approximately hydrostatic by virtue of small c_i, we infer vertical velocities from the continuity equation for two-dimensional (2D) motions given by

$$w'_w = -k u'_w/m \simeq -\omega_i u'_w/N. \tag{15}$$

This results in estimates of $w'_w \sim 0.05$ to $0.15 u'_w$. Taking the intermediate value as representative, this yields a range of vertical velocities at the sites of excitation of $w'_w \sim 0.3$ to $3\,\mathrm{m\,s^{-1}}$.

In general, the momentum flux (per unit mass, or more correctly the wave-induced Reynolds stress) for an individual wave motion may be expressed in terms of the wave parameters (again assuming hydrostatic motions) as

$$\overline{u'_w w'_w} = -\frac{k}{2m} {u'_w}^2 \simeq -\frac{\omega_i}{2N} {u'_w}^2 \simeq -\frac{k}{2N}\alpha^2 (c - \overline{u})^3, \tag{16}$$

or in terms of λ_z as

$$\overline{u'_w w'_w} \simeq -\frac{k N^2}{16\pi^3}\alpha^2 \lambda_z^3. \tag{17}$$

With the above estimates for wave scales and perturbation velocities, and assuming that anisotropy can arise in the wave spectrum due either to preferential excitation or filtering (see below), corresponding momentum fluxes may achieve values of $(\overline{u'_w w'_w})_p \sim 1$ to $100\,\mathrm{m^2\,s^{-2}}$. Here the subscript "p" denotes the local flux at the site of each convective plume, larger values accompany the larger scales at a given wave frequency, and the overbar denotes an average over the phase of the wave motion near the plume.

It is also important to note that these estimates apply only in the vicinity of penetrative convection, and that the anticipated widely distributed nature of these convective plumes will dramatically lessen the horizontally-averaged amplitudes (and momentum fluxes) of the excited wave motions. If we further assume that gravity waves are excited efficiently only by the confined descending plumes, that these plumes influence the stratified interior on spatial scales of ~ 1000 km, and that they are spaced at distances corresponding to meso-granulation scales

($\sim 10,000$ km) expected to be representative of the deeper layers within the convection zone, then the fraction of the volume experiencing wave excitation with the amplitudes and momentum fluxes estimated above is $\sim 10^{-2}$. This in turn suggests averaged momentum fluxes (for strongly anisotropic propagation) of

$$(\overline{u'_w w'_w})_a \sim 10^{-2} - 1\,\mathrm{m^2\,s^{-2}}, \tag{18}$$

where the subscript "a" denotes a horizontally-averaged value. The implications of these fluxes and of the anisotropy imposed by shear at the convective/stratified interface will be explored further below.

3.2. Excitation by shear

We now consider the potential for excitation of gravity waves in the solar interior, not by convection itself, but by the relative motion of stratified fluid within the solar interior beneath the convective plumes. As noted earlier in this section, such processes are now believed to account for appreciable gravity wave excitation in the terrestrial atmosphere and may be expected by analogy to play a similar role in the solar interior due to the tachocline spanning the convective/stratified interface. To estimate the wave scales and frequencies excited by motion beneath the "internal corrugations" imposed by penetrative convection, we rely on our previous estimates of plume penetration and the shear imposed by differential rotation. Assuming initially that the convective plumes retain the horizontal motion at the convective/stratified interface and that they occur on comparable or longer time scales relative to the shear flow, we estimate an advective velocity and time scale to be $u_s \sim S\zeta' \sim 10\,\mathrm{m\,s^{-1}}$ and $T_s \sim \lambda_h/u_s \sim \lambda_h/(S\zeta') \sim 1$ to 3 days for $\lambda_h = 1000$ and 3000 km, respectively. For our assumed plume penetrations then, the implied intrinsic phase speeds (assuming $c = 0$) and vertical scales that might arise in this manner are ~ 2 to 3 times smaller than estimated for convective penetration itself.

Estimates of amplitudes and fluxes will diverge strongly for the two mechanisms in the event that penetration depths differ significantly from the assumed value of ζ', however. Deeper penetration, for example, would lead to shear-generated waves having increased phase speeds, higher intrinsic frequencies, potentially larger wave amplitudes, and dramatically greater wave penetration into the solar interior by virtue of the strong dependence on λ_z (or c_i) in Eq. (10). An energetic plume penetrating twice the average penetration depth into the stratified interior, with other assumptions remaining the same, would imply, by Eq. (16), an $\sim 2^3$ increase in the momentum flux at the source depth, and by Eq. (10), an $\sim 2^4$ increase in the dissipation length, implying a potentially significant increase in the momentum flux at greater depths in cases where attenuation would otherwise be significant.

Thus, the dominant source mechanism and the role of gravity waves in the dynamics of the solar interior depend critically on the efficiency and extent of penetrative convection. Nevertheless, we can proceed with our current assumptions to estimate wave influences relevant for both convective and shear sources of gravity waves. The only difference at this stage is in the initial anisotropy of the wavefield and how this evolves with depth. In the case of convective excitation, the initial spectrum is presumed to be isotropic, with anisotropy (and net momentum fluxes) arising as a consequence of filtering by the mean shear, as discussed in Sect. 2. In the case of shear excitation, the initial spectrum is anisotropic since phase speeds are then imposed by the source speed ($\mathbf{c} \sim 0$). At greater depths, the waves necessarily propagate largely against the mean shear flow (with $c_i = c - \overline{u}_c \sim -\overline{u}_c > 0$ at equatorial latitudes and the reverse at high latitudes). The primary difference between these two wave sources, then, is the distribution of phase speeds accompanying each, with that due to convection likely being much broader.

Another form of shear excitation, due to unstable tachocline shear rather than flow beneath convection, has been advocated by McIntyre (1994) as possibly relevant to gravity and/or Rossby wave excitation, propagation, and mean flow interactions in the solar interior. Such radiation is believed to be a viable source of gravity waves in the terrestrial atmosphere, via either linear excitation (Sutherland & Peltier 1994) or nonlinear coupling to larger horizontal scales (Fritts 1984a; Chimonas & Grant 1984). The vertical scale of the solar tachocline suggests very large horizontal scales of instability unless these scales can be reduced significantly due, for example, to vertically-convergent motions in the vicinity of convective plumes. Such processes are nevertheless likely to occur near the convective/stratified interface, and could contribute additional gravity waves having preferred upstream (prograde, at equatorial latitudes) horizontal propagation and potentially large vertical scales, were they able to be excited efficiently. However, we confine our attention at present to those sources for which we can provide more quantitative guesses of the relevant scales and efficiencies.

4. Gravity wave filtering and momentum fluxes in the solar interior

As shown in Sect. 2, the penetration of gravity waves into the solar interior will depend on their intrinsic wave parameters, the variations of these parameters with depth, and the dissipation scales that apply in each case. Given the intrinsic phase speeds implied by the convective and shear sources we have assumed, we expect that the gravity wave spectrum will be strongly filtered by critical level processes and rapid radiative damping of the smaller vertical scales very near the depth of excitation. Gravity waves having retrograde phase speeds at equatorial latitudes $c \ll S z_s \cos\theta$, with z_s and $\cos\theta < 0$, will encounter critical levels very close to their source, thus removing them almost immediately. Likewise, waves escaping critical level absorption, but having intrinsic phase speeds that are small at some depth or that remain small by virtue of meridional rather than zonal propagation, will be strongly attenuated by radiative diffusion since $L_d \propto \omega_i^4$ from Eq. (10). Effectively, then, only those gravity waves having higher prograde phase speeds will

penetrate any significant distance below their source depth at equatorial latitudes (with the reverse at high latitudes).

Eqs. (5) to (7) also imply constraints on gravity waves having prograde (retrograde) phase speeds at equatorial (high) latitudes, as discussed in Sect. 2. As an example, a gravity wave propagating at an azimuth with $\cos\theta > 0$ will experience an increasing $c_i = c - \overline{u}_c$ with increasing depth in the prograde equatorial shear. But if $c_i > N/k$ before reaching the unsheared radiative interior, the vertical wave structure will become evanescent and the gravity wave will reflect back toward the source depth.

To quantify the penetration depths achieved by the various gravity wave scales and azimuths of propagation, we compute the fractional momentum flux remaining at depth z for the azimuths of propagation, $\theta = 0$ and $\pi/4$, subject to the assumed shear profile, gravity wave parameters, and dissipation scales discussed above. In our coordinate system, wave excitation is assumed to occur at $z_f \sim -0.1H \simeq 0.2z_s$, as this is a reasonable current estimate of the depth to which convection may penetrate. Below this depth, wave momentum fluxes will be attenuated a fraction

$$dF(z) = -(1 - e^{2dz/L_d(z)})F(z) \simeq 2dzF(z)/L_d(z) \qquad (19)$$

in each interval dz, where the factor of 2 in the exponent appears because of the quadratic dependence of the momentum flux on wave amplitude. In addition, $L_d(z)$ varies with depth due to the shear imposed by differential rotation (i.e., λ_z changes with depth). Thus, the variation of $F(z)$ with depth is given by

$$\ln F(z) - \ln F(z_f) = -\int_z^{z_f} \frac{2}{L_d(z)} dz \qquad (20)$$

for depths within the shear ($z_f > z > z_s$), where z_f denotes the depth at which the gravity waves are excited.

We now use $\omega_i = kc_i$ and Eq. (1), and again assume hydrostatic motions, to rewrite Eq. (10) in terms of the intrinsic phase speed as

$$L_d \simeq \frac{2\pi}{\kappa N^3 \lambda_h}(c - \overline{u}_c)^4 = L_0(c - \overline{u}_c)^4, \qquad (21)$$

where $L_0 = 2\pi/\kappa N^3 \lambda_h$. Then defining the remaining momentum flux at depth z for azimuth of propagation θ as $A(\theta, z) = F(z)/F(z_f)$ and using Eq. (21) with c and θ constant, Eq. (20) becomes

$$\ln A(\theta, z) = -\frac{2}{L_0}\int_z^{z_f} \frac{dz}{(c - Sz\cos\theta)^4} = \frac{2}{3L_0 S\cos\theta}\left[\frac{1}{(c - Sz\cos\theta)^3} - \frac{1}{(c - Sz_f\cos\theta)^3}\right] < 0. \qquad (22)$$

At greater depths for which L_d is constant in the absence of additional vertical shear, the cumulative remaining momentum flux is given by

$$\begin{aligned} A(\theta, z) &= A(\theta, z_s)\exp\left(-\int_z^{z_s} \frac{2}{L_d} dz\right) \\ &= A(\theta, z_s)\exp\left[\frac{-2(z_s - z)}{L_d(z_s)}\right] \text{ for } z < z_s, \end{aligned} \qquad (23)$$

with $L_d(z_s)$ defined by Eq. (10) for the parameters appropriate below the tachocline.

We are now in a position to estimate the influence of radiative diffusion on gravity wave penetration into the solar interior as a function of their intrinsic wave parameters and their azimuths of propagation. In order to span the phase speeds anticipated in Sect. 3, we consider values in the range $c = 10$ to $90\,\mathrm{m\,s^{-1}}$, with the intermediate and larger of these corresponding to the assumed horizontal wavelengths of 2000 and 3000 km. As above, we take $\overline{u}_s = 40\,\mathrm{m\,s^{-1}}$, $N = 1.2\times10^{-3}\,\mathrm{s^{-1}}$, $\lambda_h = 1000$, 2000, and 3000 km, $z_s = -0.053R_\odot \simeq -H/2$, and $z_f \simeq 0.2z_s$. If we also take $\kappa \simeq 10^3\,\mathrm{m^2\,s^{-1}}$ (Gough 1977; Press 1981; McIntyre 1994), then $L_0\overline{u}_s^4 \simeq 0.3$ to 1×10^7 m for $\lambda_h = 3000$ to 1000 km, respectively. As noted above, curves defining the loci of (c, k) values for which the fractional remaining momentum flux at z_s is e^{-1} and e^{-3} are shown for reference with dotted lines in the top panel of Fig. 2. Note that these attenuation curves are symmetric about the range of phase speeds excluded from propagation into the solar interior by critical levels, since waves on either side simply experience variations of L_d that are inverted with depth. Corresponding attenuation curves for $\overline{u}_s = 20\,\mathrm{m\,s^{-1}}$ are displayed in the lower panel of Fig. 2.

The attenuations imposed by radiative diffusion for various wavelengths and phase speeds at azimuths of propagation of $\theta = 0$ and $\pi/4$ are listed for comparison in Table 1. These attenuations emphasize what was apparent qualitatively from Eq. (21). Gravity waves having small intrinsic phase speeds at their source depth undergo severe attenuation. Only those waves having shorter periods and larger horizontal scales effectively escape strong radiative damping. These tendencies are further magnified for azimuths of propagation other than zonal and for smaller differential velocities, since in these cases prograde intrinsic phase speeds increase less rapidly with increasing depth.

In principle, those gravity waves having larger retrograde phase speeds will escape critical level absorption provided $c > \overline{u}_s$. In this case, however, c_i will decrease with depth, causing a corresponding decrease of L_d with depth, strong wave attenuation, and only minimal momentum flux surviving to the lower depths of the tachocline. This is depicted clearly in Fig. 2, where the curves and darker shading defining successively higher damping for retrograde propagation are seen to include a range of large phase speeds retrograde relative to the mean motion $\overline{u}_s$ at z_s. The same tendency is also noted for prograde propagation at small initial intrinsic phase speeds for the reason discussed above. In the case of prograde propagation, however, the assumed initial phase speeds lead to intrinsic phase speeds that are much larger and which suffer much less attenuation due to radiative damping within the tachocline.

Several things are implied by this analysis and warrant further discussion. First, as is obvious from Eq. (21), attenuation of wave momentum flux is highly sensitive to the azimuth of propagation, the magnitude of the shear, and the initial phase speeds. This attenuation has three principal effects. It insures that the gravity wave spectrum will be highly anisotropic at most latitudes, with essentially all momentum transport being downward and prograde (retrograde) at low (high) latitudes. It

Table 1. Momentum flux attenuations for the various horizontal wavelengths and phase speeds considered in the text for azimuths of propagation 0 and $\pi/4$.

	λ_h(km)								
	1000			2000			3000		
c(m/s)	10	20	30	20	40	60	30	60	90
$\overline{u}_s = 40m/s$									
$A(0, z_s)$	10^{-12}	1×10^{-3}	.075	10^{-6}	.091	.48	4×10^{-4}	.33	.73
$A(\pi/4, z_s)$	10^{-26}	10^{-5}	.016	10^{-11}	.029	.37	10^{-6}	.22	.68
$\overline{u}_s = 20m/s$									
$A(0, z_s)$	0	10^{-9}	.0027	10^{-17}	.0082	.28	10^{-8}	.15	.63
$A(\pi/4, z_s)$	0	10^{-13}	3×10^{-4}	10^{-25}	.0021	.22	10^{-11}	.10	.59

acts to further reduce the total momentum flux of the spectrum by confining the fraction that survives strong attenuation to a smaller zonal angle with increasing depth. Finally, it acts to confine significant momentum fluxes to those latitude bands where the velocity shears due to differential rotation are a maximum. The net effect is to concentrate gravity wave influences within the tachocline and below at those scales that are simultaneously excited with sufficient amplitudes to have non-negligible initial momentum fluxes and sufficiently fast (with large c, c_i, and λ_z) to survive severe attenuation by radiative diffusion.

The above examples confirm the expectations based on Eq. (21) and show clearly that only large initial (or intrinsic) phase speeds survive to appreciable depths. As noted previously, such phase speeds should arise from the temporal modulation of convection at the source depth and would have an immensely beneficial effect in terms of the subsequent penetration of these waves with minimal damping into the solar interior. On the other hand, we expect that convection will also preferentially excite gravity waves at smaller horizontal scales and phase speeds, thus leading to an optimal horizontal scale for forcing of the solar radiative interior. It would be possible to integrate over all propagation azimuths to obtain an estimate for the total surviving momentum flux for various wave parameters. But given the magnitude of the uncertainties in our knowledge of wave scales, momentum fluxes, and spectral character at present, simpler estimates seem adequate for now.

Also apparent from Eq. (21) is that the majority of the attenuation for gravity waves exiting the tachocline at $z \sim z_s$ occurs at depths immediately beneath the source depth (except for waves having $\theta \sim \pi/2$) where the initial vertical wavelengths and intrinsic phase speeds are smaller than at greater depths. To illustrate this and the above dependencies of wavelength and initial phase speed, we show depth profiles of momentum flux, normalized by the value at z_f, for $\overline{u}_s = 40$ and $20\,\mathrm{m\,s^{-1}}$, azimuth $\theta = 0, \lambda_h = 3000\,\mathrm{km}$, and $c = 30, 60,$ and $90\,\mathrm{m\,s^{-1}}$ with the dash-dotted lines in the upper and lower panels of Fig. 3. Shown for comparison in each panel are the corresponding profiles for $\lambda_h = 2000\,\mathrm{km}$ with $c = 20, 40,$ and $60\,\mathrm{m\,s^{-1}}$ (solid lines) and for $\lambda_h = 1000\,\mathrm{km}$ with $c = 10, 20,$ and $30\,\mathrm{m\,s^{-1}}$ (dashed lines). In each case, the majority of the attenuation occurs within $\sim 0.2|z_s| \sim 0.01 R_\odot$ and the stronger attenuations occur for the smaller initial phase speeds. We also note here that the attenuations would be less severe were we to account for the increasing N with depth below the convective/stratified interface. The reason for this is that a smaller N at the source depth would imply more rapid vertical propagation at just those depths where the waves are most strongly damped (see Eqs. (1) and (21)). Indeed, a linear variation in N across the velocity shear would nearly offset the shear influences in Eq. (21). Yet N appears to increase more quickly with depth (Brown et al. 1986; Zirin 1988, page 110), and without more detailed knowledge of the source mechanisms and environment there seems little value in adding further complexity at this stage.

We illustrate the influence of azimuth of wave propagation on the momentum flux remaining at $z = z_s$ for $\lambda_h = 1000\,\mathrm{km}$ (dashed lines) and $3000\,\mathrm{km}$ (dash-dotted) and for their respective initial phase speeds with $\overline{u}_s = 40$ and $20\,\mathrm{m\,s^{-1}}$ in the upper and lower panels of Fig. 4. These plots of surviving momentum flux with θ quantify the zonal focusing that accompanies azimuthal filtering of the initial gravity wave distributions and further clarify the role of large initial phase speeds in avoiding excessive gravity wave attenuation with increasing depth. The upper and lower axis labels are appropriate for high and equatorial latitudes, respectively.

A related point, noted in the previous section, is that deeper plume penetration also implies higher intrinsic frequencies, larger vertical wavelengths, and correspondingly larger momentum fluxes and dissipation lengths. Thus, very few, extreme plume penetrations might play a key role in determining the dominant gravity wave fluxes and their statistical forcing of the solar interior.

5. Downward control and the induced residual circulation

5.1. Downward control

We now examine the implications of systematic gradients of gravity wave momentum flux accompanying dissipation in a rotating, approximately geostrophically balanced fluid. The basis for this discussion are the analyses of balanced responses to wave forcing, termed "downward control" by McIntyre and colleagues (McIntyre 1989; Haynes et al. 1991). This principle derives from the zonally-averaged equations for a steady, balanced flow including the body forces accompanying wave momentum flux, or more generally Eliassen-Palm flux, diver-

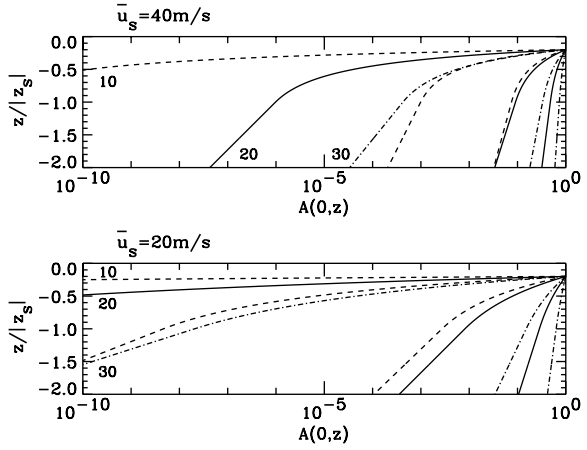

Fig. 3. Profiles of $A(0,z)$ for $\overline{u}_s = 40$ (top) and 20 m s^{-1} (bottom). Dash-dot lines display attenuation for $\lambda_h = 3000$ km and for $c = 30, 60,$ and $90\,\mathrm{m\,s^{-1}}$, with decreasing $A(0,z)$ for decreasing phase speeds. Solid lines are for $\lambda_h = 2000\,\mathrm{km}$ for $c = 20, 40,$ and $60\,\mathrm{m\,s^{-1}}$, and dashed lines are for $\lambda_h = 1000\,\mathrm{km}$ for $c = 10, 20,$ and $30\,\mathrm{m\,s^{-1}}$.

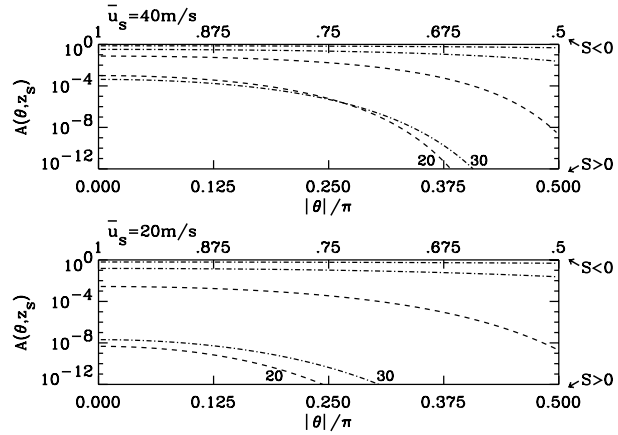

Fig. 4. As in Fig. 3, but for profiles of $A(\theta, z_s)$ for $\overline{u}_s = 40$ (top) and 20 (bottom) m s^{-1}.

gence. Assuming for our purposes that motions in the solar interior are governed only by hydrodynamic forces, the steady zonal momentum and anelastic continuity equations, neglecting diffusive effects but including wave (or eddy) stresses, may be expressed in spherical coordinates as (Haynes et al. 1991),

$$\left[\frac{1}{r\cos\phi}\frac{\partial}{\partial\phi}(\overline{u}\cos\phi) - f\right]\overline{v}^* + \left[\frac{\partial\overline{u}}{\partial z} + 2\Omega\cos\phi\right]\overline{w}^* = D_F \tag{24}$$

and

$$\frac{\overline{\rho}}{r\cos\phi}\frac{\partial}{\partial\phi}(\overline{v}^*\cos\phi) + \frac{\partial(\overline{\rho}\overline{w}^*)}{\partial z} = 0. \tag{25}$$

Here $\overline{u}$, $\overline{v}^*$, and $\overline{w}^*$ are the mean zonal and residual mean meridional and vertical velocities, $D_F \simeq -(1/\overline{\rho})\partial(\overline{\rho}\overline{u'w'})/\,\partial z$ is the body force per unit mass appropriate for gravity waves at intrinsic frequencies $\omega_i^2 \gg f^2$, $r \simeq 0.7R_\odot$ is the solar radius at the depth of wave forcing, and we have assumed that $|\partial\overline{u}/\partial r| >> \overline{u}/r$ (Tomczyk et al. 1995) and $|\Delta z/r| << 1$.

Solution of Eqs. (24) and (25) for the residual mean circulation $(\overline{v}^*, \overline{w}^*)$ requires knowledge of the (assumed steady) mean zonal velocity profile $\overline{u}(\phi, z)$. It also presumes either that there are processes acting to maintain the mean zonal velocity profile independent of the residual mean circulation or that the back effect of the residual mean circulation on the mean zonal motion is insignificant on the time scale over which this wave-driven circulation must operate. We demonstrate in the Appendix that the contribution to the mean zonal circulation induced by the residual mean circulation is a negligible fraction of $\overline{u}$ because of the very small magnitudes of the anticipated momentum fluxes and corresponding body forces. However, it is additionally possible that the tachocline structure is imposed largely by the convective processes maintaining differential rotation of the convection zone and/or magnetic influences in the solar interior (McIntyre 1994).

For solar parameters $\overline{u}_s \sim 40$ m s^{-1} (in the reference frame of the interior), $r \simeq 5 \times 10^8$ m, and $\Omega \simeq 2.7 \times 10^{-6}$ s^{-1}. Then assuming that $\overline{v}^* >> \overline{w}^*$, we see that the only significant term on the left side of Eq. (24), except at very high latitudes, is the Coriolis torque, yielding to a good approximation

$$\overline{v}^*(z) = \frac{1}{\overline{\rho}f}\frac{\partial}{\partial z}(\overline{\rho}\overline{u'w'}) \tag{26}$$

at latitudes sufficiently far from the equator.

Substituting $\overline{v}^*$ from Eq. (26) into Eq. (25) and integrating from z downward to a depth at which the momentum flux is negligible ($z \sim -2H$) yields

$$\overline{w}^*(z) \simeq -\frac{1}{r\cos\phi}\frac{\partial}{\partial\phi}\left(\frac{\cos\phi}{f}\overline{u'w'}\right), \tag{27}$$

with the same restrictions applying at equatorial latitudes. This expression is referred to as the "downward control principle" since it can be shown in the terrestrial case, where body forces accompany the upward propagation and dissipation of wave motions, that the influences of the body forces accompanying nonzero flux divergence are entirely downward for time scales sufficiently long compared to radiative relaxation times (McIntyre 1987; Haynes et al. 1991; Haynes & Shephard 1996). In the solar context, the wave stresses are themselves imposed from above and result in an induced circulation that penetrates as deeply into the solar interior as the wave momentum fluxes, though necessarily involving an ever-decreasing fraction of the solar mass as wave momentum fluxes decay. We also note that the induced circulation is likely confined to the tachocline due to differential rotation spanning the convective/ stratified interface, except for its downward extension into the solar interior accompanying gravity wave propagation and dissipation in the solar interior. A more general expression would apply were we also to consider lower-frequency gravity wave and/or Rossby wave motions or retain the terms neglected above (Haynes et al. 1991). For our purposes, however, Eq. (27) describes well the mean responses to the higher-frequency gravity waves we have envisioned here.

We have neglected the effects of thermal diffusion in the preceding calculation in order to describe the potential influences of gravity wave forcing in the solar interior as simply as possible. We note, however, that thermal diffusion could act to alter the residual mean circulation and the implied transport of fluid within the outer radiative interior of the Sun in ways not known at present. Nevertheless, we know in the terrestrial context that wave forcing and the "downward control" mechanism lead to large departures from radiative equilibrium conditions (required for a balanced flow including wave forcing) without suppressing the residual mean circulation accounting for these departures (Garcia 1989; McIntyre 1989). We also have shown in the Appendix that the wave-driven residual mean circulation has a negligible influence on the mean zonal circulation. Therefore, we expect that other processes which might lead to the evolution or spreading of the tachocline structure would lead to gradual changes in gravity wave excitation, propagation, and filtering without changing the implications of gravity wave forcing for a residual mean circulation and Lithium depletion in the solar interior. We are currently developing a numerical model of the solar interior and lower convection zone to explore these and other generalizations of our analytic solutions more completely.

5.2. The induced residual circulation

For any assumed gravity wave scales, initial momentum flux, and azimuth of propagation, the attenuation accompanying downward propagation is described by Eqs. (22) and (23) within and below the tachocline, respectively. As noted above, however, strong azimuthal filtering (the preferential removal of waves having smaller c_i and λ_z) causes the remaining wave spectrum to become increasingly narrow in its propagation azimuth about $\theta = 0$ ($\theta = \pi$) at equatorial (high) latitudes with increasing depth. This azimuthal filtering further reduces the total momentum flux available to influence solar interior dynamics relative to that inferred for strictly zonal propagation. The total momentum flux at any depth represents an integration over the remaining momentum fluxes for each azimuth of propagation. Eqs. (26) and (27) then allow us to use the resulting momentum flux profiles to compute the corresponding residual circulation $(\overline{v}^*, \overline{w}^*)$ throughout the solar interior at latitudes away from the equator.

Based on our discussion of plausible gravity wave sources in Sect. 3, we assume that the excited wave spectrum either has initially, or rapidly achieves, a high degree of anisotropy in the azimuth of wave propagation, with primarily prograde (retrograde) phase speeds of ~ 10 to $100\,\mathrm{m\,s^{-1}}$ relative to the convective/stratified interface at low (high) latitudes. This implies comparable or larger intrinsic phase speeds at the source depth ($z_f \sim -0.1\,\mathrm{H} \sim 0.2 z_s$), with the larger of these more easily overcoming attenuation due to small dissipation scales, L_d. These assumptions also imply momentum flux profiles which exhibit significant attenuation with increasing depth, with the majority of the wave dissipation, and the accompanying momentum flux divergence, occurring at depths immediately below the source depth.

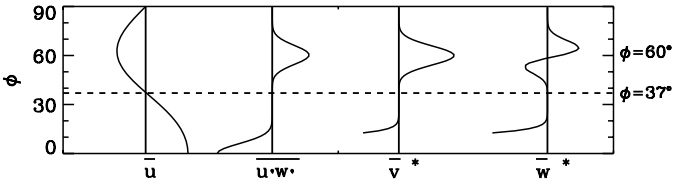

Fig. 5. Schematic of latitudinal distributions of zonal convection velocities relative to the interior, the gravity wave momentum flux at z_s inferred in the text, and the corresponding $\overline{v}^*$ and $\overline{w}^*$ (from left to right).

With negative momentum fluxes (corresponding to downward transport of prograde momentum) at equatorial latitudes, and the reverse at high latitudes, we have both horizontal and vertical momentum flux gradients which specify the wave-driven residual circulation through Eqs. (26) and (27). Our hypothesized latitudinal distribution of gravity wave (or convective) momentum flux and the implied distributions of $\overline{v}^*$ and $\overline{w}^*$ with latitude are shown in Fig. 5. The corresponding circulation in a latitude-height plane is depicted in Fig. 6. The momentum flux distribution with latitude is mirrored qualitatively by $\overline{v}^*$ via Eq. (26) at extra-equatorial latitudes because the momentum flux and its vertical gradient are expected to be correlated. This does not apply at equatorial latitudes, however, where the assumption of steady motion and a quasi-geostrophic balance is no longer valid. The positive (negative) momentum flux gradients with latitude equatorward (poleward) of $\phi \sim 60^o$ likewise imply via Eq. (27) mean vertical motions $\overline{w}^*$ that are downward (upward) equatorward (poleward) of $\phi \sim 60^o$. As above, however, violation of quasi-geostrophic assumptions at equatorial latitudes invalidates Eq. (27) in that region. The overall sense of the wave-driven circulation, then, is subsidence at low and middle latitudes, divergent meridional flow about the reversal in momentum flux with latitude, and rising motions at high latitudes and (presumably, from continuity) at equatorial latitudes at which Eqs. (26) and (27) provide no guidance. Because the momentum fluxes and their gradients decrease with depth, the induced circulation decays accordingly.

While qualitative, there are some obvious implications as well of the strong dependence of L_d on c_i and thus on $\overline{u}_s$ with latitude. As demonstrated for differential velocities of 40 and $20\,\mathrm{m\,s^{-1}}$, smaller shears lead to much smaller intrinsic prograde (retrograde) phase speeds at low (high) latitudes and to correspondingly greater attenuations of the momentum flux for all but the highest phase speeds. This implies much narrower distributions of momentum flux with latitude within and below z_s than of the shears imposed by differential rotation. From Eqs. (26) and (27), we see that confining significant momentum fluxes to narrow latitude bands likewise restricts the latitudinal extent of the wave-induced residual circulation, with $\overline{v}^*$ important only where momentum fluxes (and vertical gradients) are significant and with maximum upwelling or subsidence occurring at the edges of these narrower bands of wave forcing. The result, if our assumptions of wave scales and attenuations are reasonable, is a residual circulation having two cells in each hemisphere. One

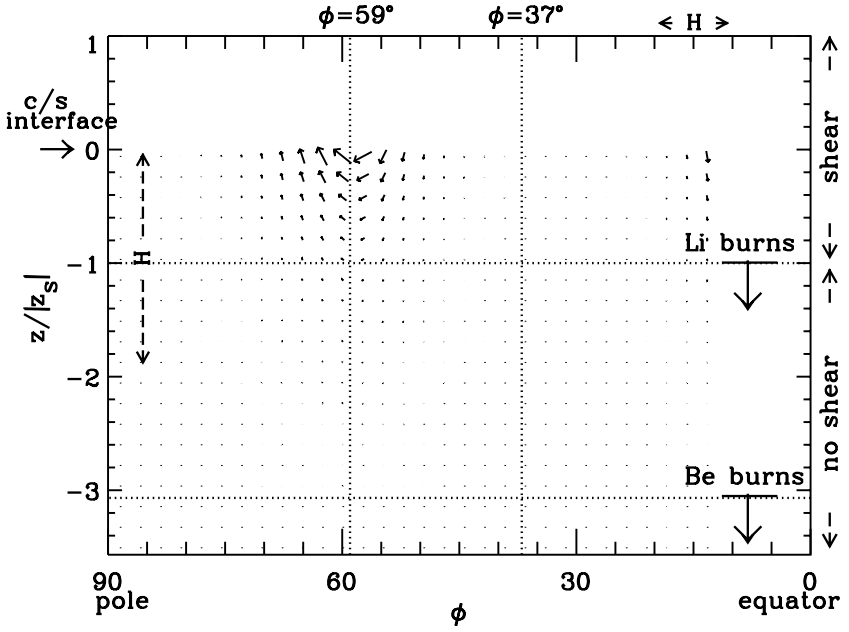

Fig. 6. The hypothesized residual circulation in a latitude-height plane. Note that $\overline{v}^*$ and $\overline{w}^*$ are anticipated to be maximum where the momentum fluxes and their gradients are large and that Eqs. (26) and (27) cannot be used to infer the circulation at equatorial latitudes where the flow is neither steady nor quasi-geostrophic. The vertical component of the induced residual circulation is enhanced by a factor of 10 for illustration purposes.

cell is confined at low latitudes with maximum subsidence at $\phi \sim 20^o$ and equatorward meridional flow at lower latitudes. A second cell is centered near the latitude of maximum retrograde shear ($\sim 60^o$) and exhibits subsidence on the equatorward edge, poleward flow at the latitude of maximum momentum flux, and upwelling at the poleward edge. The implied circulation is thus more confined in latitude than the variations in shear due to differential rotation, but is also stronger by virtue of the larger vertical motions (and larger latitudinal gradients of momentum flux) accompanying this latitudinal localization.

Another variation to consider here are the possible consequences of reversed vertical gradients of momentum flux near the convective/stratified interface. We might suppose somewhat different gravity wave excitation or filtering scenarios having different implications for flux gradients (and their implied residual circulations). We note, for example, that Eq. (26) implies a reversal of the meridional circulation at the depth at which the vertical gradient of the density-weighted Reynolds stress, $\partial(\overline{\rho}\overline{u'w'})/\partial z$, changes sign. Such a reversal could occur, provided the operative gravity wave sources excited a wave spectrum having approximately isotropic azimuths of propagation initially which were subsequently filtered to cause an initial increase in the momentum flux magnitude with depth. In this event, the wave-driven circulation would largely close below the convective/stratified interface and would have reversed meridional motions in the shallow layer in which the gravity wave filtering occurred. Such momentum flux profiles would also imply smaller vertical velocities across the convective/stratified interface and less exchange of mass between the convection zone and the stratified interior. The implications for the dynamics of the solar interior would remain largely unchanged, however, provided the net flux emerging beneath the source depth is of the same sign and of comparable magnitude.

6. Implications for lithium and beryllium concentrations

We now attempt to quantify the implications of the wave-driven residual circulation postulated above for depletion, or lack of, of Lithium and Beryllium. To do so, we must use our estimates of momentum flux at the source depth and of attenuation at greater depths to anticipate the time scales required for overturning of the solar interior to depths at which these elements are destroyed. Such a procedure involves several aspects which we will attempt to identify and quantify separately. First, we must quantify the momentum flux attenuation, as this will impose the mean vertical motion at each depth. Second, we must determine the time scale for overturning to burning depths. Third, we must estimate the fraction of the fluid penetrating to these depths during each overturning, since much of the residual circulation may be confined to shallower depths if damping scales are small. Finally, we must estimate the number of overturnings required, given the above, to account for the observed levels of Lithium and Beryllium depletions ($\sim 99\%$ and small, respectively).

Time scales on which Lithium and Beryllium are destroyed in the solar interior exhibit strong dependencies on temperature and solar species densities. Reported values for the temperature at which Lithium burns range from 2.4 to 2.7×10^6 K (Foukal 1990), while thermonuclear reaction rate calculations indicate that Lithium destruction time scales decrease sharply with increasing temperature or decreasing solar radius (Caughlan & Fowler 1988; J. Guzik and F. Swenson, private communication, 1997). The relevant temperatures for Beryllium are $\sim 3.5 \times 10^6$ K and imply depths approximately a scale height deeper than for Lithium. The temperature range reported for Lithium implies burning radii below $r_{Li} \sim 0.66\, R_\odot$, while the initial radius for Beryllium is $r_{Be} \sim 0.55\, R_\odot$ or deeper. Thus, we will assume for our purposes here that the appropriate values are $0.66\, R_\odot$ and $0.55\, R_\odot$, respectively, but recognize that transport to greater depths significantly increases the burning

rates (though the uncertainties do not affect our plausibility arguments greatly).

Now also take as given our estimate of the horizontally-averaged momentum flux that can be generated by convective plumes penetrating ~ 0.1 H into the stratified interior, $(\overline{u'_w w'_w})_a \sim 10^{-2}$ to 1 m^2 s^{-2}. We then assume that the central decade of this estimate is the most probable, i.e., ~ 0.03 to 0.3 m^2 s^{-2}. We further assume that this momentum flux is distributed approximately uniformly in azimuth and among the various wave scales and frequencies discussed above.

That portion assigned to smaller scales and initial phase speeds will be preferentially attenuated at relatively shallow depths beneath the source depth and will play no role in Lithium depletion. The fraction not severely attenuated will depend on the initial distribution of amplitudes, wavelengths, and phase speeds, but will likely be a small fraction, ~ 0.3 or less, given the strong attenuation at the smaller assumed scales. The zonal momentum flux per unit mass for this fraction will be further reduced by radiative diffusion, zonal focusing, and the decreases accompanying density increases with increasing depth, since $\overline{\rho u' w'}$ is constant in the absence of wave dissipation. From Table 1 and Figs. 3 and 4, we see that radiative damping and zonal focusing together will contribute an additional reduction of ~ 0.03 to 0.3, depending on λ_h and c. An increasing mean density below z_f will impose a further reduction. Assuming that fluid must be transported to depths below the nominal burning depth for lithium, z_{Li} (the burning depth measured relative to the convective/stratified interface), this implies a further decrease of $e^{-0.5}$, and cumulative additional flux reductions will then be ~ 0.005 to 0.05. Again taking an intermediate value of 0.02, the momentum flux surviving to z_{Li} at the latitudes of maximum tachocline shear will be $\overline{u'w'} \sim 6$ to 60 $\times 10^{-4}$ m^2 s^{-2}. These values imply, from Eq. (27), residual mean vertical velocities $\overline{w}^*$ at z_{Li} that are likewise smaller by the same factors.

The time scale for the residual circulation to a particular depth is specified most generally by integrating along the Lagrangian trajectories of fluid parcels achieving this depth. In cases where the residual circulation is not known precisely, however, a simple estimate of the time required for vertical advection of material from the source depth z_f to z_{Li} is given by

$$T_w = \int_{z_{Li}}^{z_f} \frac{dz}{|\overline{w}^*(z)|}, \tag{28}$$

assuming that $\overline{w}^*(z)$ has the same sign at all depths, which is true for momentum flux magnitudes decreasing with depth. Note that $\overline{w}^*$ depends on latitudinal gradients which are difficult to quantify without specific knowledge of the latitudinal variations of $\overline{u'w'}$. Negative momentum fluxes achieve their maximum values at low latitudes for which tachocline shear is large and prograde with z. Positive momentum fluxes likewise maximize near the latitude at which the high-latitude shears are large and negative ($\phi \sim 60^o$). Near the transition from prograde to retrograde zonal motion of the convection zone, however, shears are small and all reasonable wave scales are strongly attenuated. Thus, gradients of momentum flux with latitude are not uniform and may, in fact, be highly localized. Since the distribution of initial phase speeds is not known, we can only guess at these gradients at this stage. Nevertheless, the result is not sensitive to the guess since a broader distribution will imply smaller, but more latitudinally extended, regions of subsidence and upwelling, with comparable implications for overturning time scales.

Under the above assumptions, the latitudinal variations of $\overline{u'w'}$ dominate those of $\cos\phi/f$. Thus, we may estimate $\overline{w}^*$ at these latitudes and at z_{Li} as

$$\overline{w}^*(z) \simeq -\frac{1}{r\cos\phi}\frac{\partial}{\partial\phi}\left(\frac{\cos\phi}{f}\overline{u'w'}\right) \sim -\frac{1}{f}\frac{\overline{u'w'}}{\Delta y}, \tag{29}$$

where $\Delta y \sim 0.05 r_{Li} \sim 2.5\times10^7$ m. For the values cited above, and assuming a latitude of 60^o, this leads to estimates of $\overline{w}^*_{Li} \sim 5$ to 50×10^{-6} m s^{-1}. Comparable values are expected at low latitudes, to the extent that downward control has the same influences when rotational influences are weaker. Assuming then that the mean value of $\overline{w}^*$ between z_f and z_{Li} is larger by ~ 1.5 (since $\overline{w}^*$ decreases rapidly initially, but decreases more gradually throughout the remainder of the tachocline), this yields estimates for the vertical transport time of $T_w \sim 10^4$ to 10^5 years. Since meridional transports accompany the vertical branches of the induced residual circulation, the overturning time scale is approximately $T_o \sim 2T_w \sim 2\times10^4$ to 2×10^5 years.

It remains only to estimate 1) the fraction, ξ, of the fluid at depths less than z_{Li} that participates in overturning to depths below z_{Li} and 2) the fraction of Lithium destroyed during each overturning cycle. The fraction transported to depths below z_{Li} is given by the product of the fraction of the mass flux that survives to z_{Li}, $(\overline{\rho w}^*)_{z_{Li}}/\ (\overline{\rho w}^*)_{z_f}$, and the fraction of the fluid volume, b, that participates in each overturning cycle at shallower depths due to the confined latitudinal extent of the induced residual circulation. With the fractional mass flux $\overline{\rho w}^*$ decreasing by ~ 0.1 or less and $b \sim 0.1$, this yields $\xi \sim 0.01$. Assuming also that fluid is transported sufficiently below z_{Li} that a fraction $\delta \sim 0.01$ of the Lithium is destroyed during each cycle due to the rapid increases of the reaction rate coefficients with temperature (typically ~ 5 to 40 across a depth of H/2, apart from density effects), then the number of overturning cycles, n, required to account for the observed Lithium depletion is given by $e^{-n\xi\delta} \sim 0.01$, since Lithium is observed to be $\sim 99\%$ depleted. This implies $n \sim 500/\delta$, or a time scale for Lithium depletion of $T_{Li} \sim 10^9$ to 10^{10} years. Thus, plausible gravity wave excitation at the convective/stratified interface appears to impose a residual circulation within the solar interior that could account for the observed Lithium depletion on a time scale of the age of the Sun.

A corresponding estimate of the overturning time required for transport to the depth at which Beryllium is destroyed, $r_{Be} < 0.55\ R_\odot$ ($\sim$ one scale height below z_{Li}), shows that 1) $\overline{u'w'}$ (and thus $\overline{w}^*$) are smaller by ~ 10 or more due to radiative diffusion and scale height effects and 2) the fraction of the outer fluid participating in overturning is further reduced by ~ 3 or more. The implication for Beryllium depletion of e^{-1} is then a number of overturnings n, with $n\xi\delta \sim 1$ and $\xi < 0.01/30$, or $n > 3000/\delta$ and $T_{Be} > 10^{10}$ to 10^{11} years. This is longer

than the solar age and suggests minimal Beryllium depletion, again consistent with observations within the uncertainties of our assumptions.

7. Summary and conclusions

We have presented a simple conceptual model of the convective excitation, azimuthal filtering, and dissipation of gravity waves in the outer radiative interior of the Sun. Convective time scales were suggested to account for horizontal phase speeds of $c \sim 10$ to $100\,\mathrm{m\,s^{-1}}$ at horizontal wavelengths of $\lambda_h \sim 1000$ to $3000\,\mathrm{km}$. The subsequent radial propagation of these motions in the shears imposed by differential rotation were inferred to lead to strong azimuthal filtering of the wave spectrum. The consequence of filtering and radiative diffusion is believed to be a tendency for predominant prograde propagation of waves (having negative zonal momentum fluxes) beneath the prograde convection at equatorial latitudes and for retrograde propagation (with positive zonal momentum fluxes) beneath the retrograde convection at higher latitudes. Attenuation of these gravity waves and their attendant momentum fluxes by radiative diffusion at greater depths then leads to zonal body forces that are prograde (retrograde) at equatorial (high) latitudes. The implications for an approximately geostrophically-balanced fluid are a wave-driven residual circulation in the meridional-vertical plane that provides the Coriolis torques required to balance the applied body forces and induces an overturning of the outer radiative interior of the Sun.

Estimates of gravity wave amplitudes and momentum fluxes due to the strength, time scales, and distributed nature of convective excitation then led to estimates of overturning times of $T_o \sim 2\times10^4$ to 2×10^5 years. Accounting both for the fraction of the fluid at shallower depths participating in such a circulation and for the number of overturnings required to achieve the observed degree of Lithium depletion resulted in an estimate of the time scale for Lithium depletion of $T_{Li} \sim 10^9$ to 10^{10} years which is in reasonable agreement with the age of the Sun, i.e., 4.6 billion years (Soderblom et al. 1993). A corresponding estimate of the time scale for depletion of Beryllium by e^{-1} yielded $T_{Be} > 10^{10}$ to 10^{11} years, and is again consistent with observations of minimal Beryllium depletion. Importantly, while the numbers provided represent crude estimates of plausible gravity wave effects, the implications for relative depletions of Lithium and Beryllium are insensitive to the magnitude of the wave forcing. Lithium is preferentially depleted because the induced residual circulation is largely confined to the shallowest depths of the radiative interior by strong radiative damping of the gravity waves excited by penetrative convection. Indeed, the penetration of the solar tachocline to approximately the depth at which Lithium is destroyed may be viewed as a manifestation of this dynamical influence.

The mechanism for Lithium depletion proposed here also has implications for Lithium observations in other stars. Two quotes by Foukal (1990) are worthy of note in this regard. He states on page 197 “Lithium depletion tends to decrease in younger main sequence stars, implying that it is not simply a result of pre-main sequence events.” Foukal (1990) also writes on page 441 “Stellar structure theory predicts that main sequence stars somewhat more massive than the Sun should be in radiative equilibrium. Such stars only develop significant convection zones after they evolve off the main sequence. Observations confirm that stellar Lithium abundances are relatively high in the more massive main sequence stars and decrease off the main sequence for these stars” (see also Soderblom et al. 1993). Finally, Lithium depletion is observed to be suppressed in stars approximately the same age as the Sun, but exhibiting faster rotation (Soderblom et al. 1993). The second quote by Foukal (1990) suggests that Lithium depletion accompanies the presence of a convection zone at larger radii only following the main sequence evolution. The first quote suggests in addition that Lithium depletion progresses with the age of a star following the main sequence. Our conceptual model is consistent with both of these statements in that 1) convection and differential rotation are fundamental to the excitation and preferential radial propagation of the gravity waves responsible for a residual circulation in a stellar interior and 2) Lithium depletion must depend on the time interval over which such a circulation has acted. The final observation that Lithium is less depleted in more rapidly rotating stars is likewise consistent with our conceptual model. There are (at least) two reasons for this dependence. First, as noted by Julien et al. (1996b), penetrative convection is strongly suppressed by rapid rotation, potentially diminishing the excitation of gravity waves in stars experiencing rapid rotation. A second reason is that the residual circulation itself is weaker for a given level of wave forcing when rotation is more rapid. This can easily be seen from Eqs. (26) and (27), which show the strength of the residual circulation required to balance the body forces due to gravity wave momentum flux gradients to be inversely proportional to the Coriolis parameter f. The implications are smaller Lithium depletions relative to Beryllium when rotation is more rapid.

Our model development has been based, as much as possible, on existing theories of gravity wave excitation, propagation, dissipation, and wave-mean flow interactions in stratified and sheared fluids. In this regard, terrestrial analogs have provided key guidance and constraints on wave scales, momentum fluxes, and shear influences. We have also relied on observations, models, and theoretical developments aimed more specifically at the convective/stratified interface or the interior structure of the Sun. However, we have necessarily made assumptions in many areas, leading to a broad range of possible forcing magnitudes and time scales for gravity wave influences in the solar interior. We have also excluded the effects of thermal diffusion on the induced residual mean circulation and possible time dependence of the mean zonal circulation and its implications for gravity wave excitation and influences. Nevertheless, we believe the results presented here make a very plausible case for gravity wave excitation, filtering, and wave-mean flow interactions having significant, if long-term, influences in the radiative interior of the Sun. If these ideas are qualitatively correct, then they should also apply to the evolutions of other stars. The additional effects of wave filtering, preferential prograde or retrograde propagation,

and the residual circulation arising from wave forcing considered in this study may have additional implications for solar interior evolutions which have not been examined to date. If so, gravity wave processes in stratified and sheared fluids may eventually be recognized to account for a number of astrophysical observations unexplained by other mechanisms already explored.

Acknowledgements. The authors benefited from valuable discussions with Joe Werne, Keith Julien, Bo Andersen, Steve Tomczyk, Steve Arendt, Michael McIntyre, Joyce Guzik and Joe Isler. We would also like to thank our reviewer J.-P. Zahn for his many thoughtful comments. Support for this research was provided by the Radio Atmospheric Science Center of Kyoto University, Kyoto, Japan, the Forsvarets Forskningsinstitutt, Kjeller, Norway, and the National Aeronautics and Space Administration under grant NAG5-5029.

Appendix

We show here that the gravity wave momentum fluxes postulated in this paper to exist in the solar interior lead to corrections to the mean zonal velocity that are insignificant relative to the large-scale flow in the tachocline. This derivation validates the assumption of a steady zonal and residual mean circulation in Sect. *5.1* and the implied character of this circulation described in Sect. *5.2*.

We first derive the spin-up solutions for the meridional and zonal circulation velocities and calculate their values assuming they have reached steady state. We then verify the steady-state assumption by confirming that the change in the mean zonal velocity is negligible for the magnitude of the wave forcing envisioned to occur in the solar interior.

Writing $\overline{u} = \overline{u}_s + \overline{u}_{rc}$, where $\overline{u}_s$ is assumed steady and $(\overline{u}_{rc}, \overline{v}^*, \overline{w}^*)$ is the spin-up residual circulation due to wave forcing, the zonally-averaged zonal and meridional momentum equations may be written

$$\begin{aligned}
\frac{\partial \overline{u}_{rc}}{\partial t} \; + \; (\mathbf{v}.\nabla)\overline{u}_{rc} + \frac{\overline{w}^*\overline{u}_{rc}}{r} - \frac{\tan\phi \overline{v}^*\overline{u}_{rc}}{r} = \\
2\Omega(-\cos\phi\overline{w}^* + \sin\phi\overline{v}^*) + D_F \\
\frac{\partial \overline{v}^*}{\partial t} \; + \; (\mathbf{v}.\nabla)\overline{v}^* + \frac{\overline{w}^*\overline{v}^*}{r} + \frac{\tan\phi\overline{u}_{rc}^2}{r} = -\frac{1}{\rho r}\frac{\partial(\overline{p}+\overline{p}_{rc})}{\partial\phi} \\
-\Omega^2 r\sin\phi\cos\phi - 2\Omega\sin\phi\,\overline{u}_{rc}, \qquad (30)
\end{aligned}$$

where $\mathbf{v}.\nabla = \overline{w}^*\partial/\partial r + \overline{v}^*\partial/\partial\phi$ and $\overline{p}$ and $\overline{p}_{rc}$ are the mean pressure of the undisturbed flow and that due to wave forcing.

Now consider a fluid which is initially at rest with respect to the rotating state and to which the body force D_F is applied at $t = 0$. Because the mean pressure gradient balances the centrifugal acceleration in the meridional momentum equation, $1/(\overline{\rho}r)\partial\overline{p}/\partial\phi = -\Omega^2 r\sin\phi\cos\phi$, we can neglect these terms at early times. Scaling indicates that we can also neglect the nonlinear advection terms, the Coriolis torques acting on the residual circulation, and the pressure gradient associated with the residual circulation. These approximations are confirmed by preliminary numerical solutions of the spin-up equations. The simplified spin-up equations are then

$$\frac{\partial \overline{u}_{rc}}{\partial t} \simeq D_F \text{ and } \frac{\partial \overline{v}^*}{\partial t} \simeq -2\Omega\sin\phi\,\overline{u}_{rc}, \qquad (31)$$

and lead to the spin-up solutions $\overline{u}_{rc} \simeq D_F t$ and $\overline{v}^* \simeq -\Omega\sin\phi\; D_F t^2$. Steady state is reached when Eq. (26) is satisfied, $\overline{v}^* \simeq -D_F/f$. Equating the two expressions for $\overline{v}^*$ then, we find that the time to reach steady state is approximately $t_{ss} \simeq \sqrt{2}/f$ (i.e., of order the solar rotation time), so that the induced mean zonal velocity at steady state is

$$\overline{u}_{rc} \simeq \sqrt{2}D_F/f. \qquad (32)$$

Note in addition that the induced zonal and meridional velocities at steady state are comparable, with $\overline{u}_{rc} \simeq -\sqrt{2}\overline{v}^*$.

As in the main body of the paper, we assume a rotation rate $\Omega = 2.7\times10^{-6}$ s^{-1} and a differential rotation velocity $\overline{u}_s$ = 40 m s^{-1}. We then estimate the body force as

$$D_F \simeq -\frac{1}{\overline{\rho}}\frac{\partial(\overline{\rho}\overline{u'w'})}{\partial z} \sim \frac{\overline{u'w'}}{z_s}, \qquad (33)$$

where $z_s = -.05R_\odot$ and the averaged momentum fluxes are $\overline{u'w'} \sim 10^{-2}$ to 1 m^2 s^{-2}. Using these values and Eq. (32), the ratio of the induced mean zonal velocity to the mean shear velocity is

$$\frac{\overline{u}_{rc}}{\overline{u}_s} \sim 10^{-6} - 10^{-4} \qquad (34)$$

at latitudes of maximum shear. Thus, wave forcing of a residual circulation in the solar interior can occur with negligible feedback on the mean zonal motion field.

References

Alexander, J.M., Holton, J.R., Durran, D.R., 1995, J. Atmos Sci. 52, 2212
Alexander, J.M., Pfister, L., 1995, Geophys. Res. Lett. 22, 2029
Andersen, B.N., 1996, A&AS 312, 610
Andreassen, Ø., Wasberg, C.E., Fritts, D.C., et al., 1994, J. Geophys. Res. 99, 8095
Arendt, S., 1993, Geophys. Astrophys. Fluid Dyn. 68, 59
Balachandran, S., Lambert, D.L., Stauffer, J.R., 1988, ApJ 333, 267
Basu, S., Anita, H.M., Narasimha, D., 1994, MNRAS 267, 209
Bonin, P., Rieutord, M., 1996, A&AS 310, 221
Brown, T.M., Mihalas, B.W., Rhodes Jr, E.J., 1986, Solar Waves and Oscillations, in: Physics of the Sun, eds. P. A. Sturrock, T. E. Holzer, D. M. Mihalas et al., vol I, D. Reidel Publ. Co., Holland
Butler, R.P., Cohen, R.D., Duncan, D.K., et al., 1987, ApJ 319, L19
Cattaneo, F., Brummel, N.H., Toomre, J., et al., 1991, ApJ 370, 282
Caughlan, G.R., Fowler, W.A., 1988, Atm. Nucl. Data Tables 40, 283
Chaboyer, B., Zahn, J.-P., 1992, A&AS 253, 173
Chaboyer, B., Demarque, P., Pinsonneault, M.H., 1995, ApJ 441, 865
Charbonneau, P., Tomczyk, S., Schou, J., et al., The Rotation of the Solar Core Inferred by Genetic Forward Modeling, 1997, submitted to ApJ
Chimonas, G., Grant, J.R., 1984, J. Atmos. Sci. 41, 2269
Christensen–Dalsgaard, J., Gough, D.O., Thompson, M.J., 1991, ApJ 378, 413

Christensen–Dalsgaard, J., Däppen, W., Ajukov, S.V., et al., 1996, Sci 272, 1286
Clark, T.L., Hauf, T., Kuettner, J.P., 1986, Quart. J. Roy. Meteorol. Soc. 112, 899
Clayton, D.D., 1983, Principles of Stellar Evolution and Nucleosynthesis, The University of Chicago Press, Chicago
Eckermann, S.D., Marks, C.J., 1996, J. Geophys. Res. 101, 21195
Foukal, P., 1990, Solar Astrophysics, John Wiley & Sons, New York
Fovell, R., Durran, D.R., Holton, J.R., 1992, J. Atmos. Sci. 49, 1427
Fritts, D.C., 1984a, J. Atmos. Sci. 41, 524
Fritts, D.C., 1984b, Rev. Geophys. Space Phys. 22, 275
Fritts, D.C., Isler, J.R., Andreassen, Ø., 1994, J. Geophys. Res. 99, 8109
Fritts, D.C., Luo, Z., 1995, J. Geophys. Res. 100, 3119
Fritts, D.C., VanZandt, T.E., 1993, J. Atmos. Sci. 50, 3685
Fritts, D.C., Vincent, R.A., 1987, J. Atmos. Sci. 44, 605
Fritts, D.C., Yuan, L., 1989, J. Atmos. Sci. 46, 2569
Garcia, R.R., 1989, J. Geophys. Res. 94, 14605
Garcia, R.R., Boville, B.A., 1994, J. Atmos. Sci. 51, 2238
García López, R.J., Rebolo, R., Magazzù, A., et al., 1991, Mem. Soc. Astron. Ital. 62, 187
Goode, P.R., Dziembowski, W.A., Korzennik, S.G., et al., 1991, ApJ 367, 649
Gossard, E.E., Hooke, W.H., 1975, Waves in the Atmosphere, Elsevier, New York, p. 456
Gough, D.O., 1977, Random Remarks on Solar Hydrodynamics, in: The Energy Balance and Hydrodynamics of the Solar Chromoshpere and Corona, eds. R. M. Bonnet and P. Delache, G. deBussae Publ.
Gough, D.O., Kosovichev, A.G., Toomre, J., et al., 1996, Sci 272, 1296
Guzik, J.A., Cox, A.N., 1995, ApJ 448, 905
Guzik, J.A., Deupree, R.G., 1996, Two-dimensional Solar Evolution Models, in: IAU Symposium 181: Sounding Solar and Stellar Interiors, IAU
Hauf, T., Clark, T.L., 1989, Quart. J. Roy. Meteorol. Soc. 115, 309
Haynes, P.H., Marks, C.J., McIntyre, M.E., et al., 1991, J. Atmos. Sci. 48, 651
Haynes, P.H., Shephard, T.G., 1996, J. Atmos. Sci. 53, 2105
Holton, J.R., 1983, J. Atmos. Sci. 40, 2497
Huebner, W.F., 1986, Atomic and Radiative Processes in the Solar Interior, in: Physics of the Sun, eds. P. A. Sturrock, T. E. Holzer, D. M. Mihalas, et al., vol I, D. Reidel Publ. Co., Holland
Hurlburt, N.E., Toomre, J., Massaguer, J.M., 1986, ApJ 311, 563
Hurlburt, N.E., Toomre, J., Massaguer, J.M., et al, 1994, ApJ 421, 245
Julien, K.A., Legg, S., McWilliams, J., et al., 1996a, Dyn. Atmos. Oceans 24, 237
Julien, K.A., Werne, J.A., McWilliams, J., et al., 1996b, The Effect of Rotation on Convective Overshoot, in: Solar Convection and Oscillations, eds. J. Christensen–Dalsgaard and F. P. Pipjers, Kluwer Academic Publishers
Knobloch, E., 1991, Towards a Theory of Wave Transport, in: Challenges to Theories of the Structure of Moderate–Mass Stars, eds. D. O. Gough and J. Toomre, Springer–Verlag, New York, p. 241–246
Kumar, P., Quataert, E.J., Bahcall, J.N., 1996, ApJ 458, L83
McIntyre, M.E., 1987, Dynamics and Tracer Transport in the Middle Atmosphere: An Overview of Some Recent Developments, in: Transport Processes in the Middle Atmosphere, eds. G. Visconti and R. Garcia, D. Reidel Publ. Co., Holland, p. 267–296
McIntyre, M.E., 1989, J. Geophys. Res. 94, 14617
McIntyre, M.E., 1994, The Quasi-Biennial Oscillation (QBO): Some Points about the Terrestrial QBO and the Possibility of Related Phenomena in the Solar Interior, in: The Solar Engine and its Influence on Terrestrial Atmosphere and Climate, ed. E. Nesme–Ribes, Springer–Verlag, p. 293–320
Pallé, P.L., 1991, Adv. Space Res. 11, 29
Pfister, L., Starr, W., Craig, R., et al., 1986, J. Atmos. Sci. 43, 3210
Press, W.H., 1981, ApJ 245, 286
Press, W.H., Rybicki, G.B., 1981, ApJ 248, 751
Rast, M.P., 1997, Solar Granulation a Surface Phenomenon, in: Geophysical and Astrophysical Convection, eds. P. Fox and R. M. Kerr, Gordon and Breach Science Publishers
Rebolo, R., Beckman, J.E., 1988, A&AS 201, 267
Rieutord, M., Zahn, J.-P., 1995, A&AS 296, 127
Schatzman, E., 1993, A&AS 279, 431
Schmitt, J.H.M.M., Rosner, R., Bohn, H.U., 1984, ApJ 282, 316
Soderblom, D.R., Jones, B.F., Balachandran, S., et al., 1993, AJ 106, 1059
Sutherland, B.R., Peltier, W.R., 1994, Phys. Fluids 6, 1267
Swenson, F.J., Faulkner, J., 1991, Main–Sequence Mass–Loss: Lithium Dilution in the Hyades and the Sun, in: Challenges to Theories of the Structure of Moderate–Mass Stars, eds. D. O. Gough and J. Toomre, Springer–Verlag, New York, p. 345–352
Swenson, F.J., Faulkner, J., 1992, ApJ 395, 654
Taylor, M.J., Hapgood, M.A., 1988, Planet. Space Sci. 36, 975
Thompson, D.J., Maclennan, C.G., Lanzerotti, L.J., 1995, Nat 376, 139
Thompson, M.J., Toomre, J, Anderson, E.R., et al., 1996, Sci 272, 1300
Tomczyk, S., Schou, J., Thomson, M.J., 1995, ApJ 448, L57
Townsend, A.A., 1965, J. Fluid Mech. 22, 241
Tsuda, T., Murayama, Y., Yamamoto, M., et al., 1990, Geophys. Res. Lett. 17, 725
Turck-Chièze, S., Däppen, W., Fossat, E., et al., 1993, Physics Reports 230, 57
Vincent, R.A., Reid, I.M., 1983, J. Atmos Sci. 40, 1321
Winters, K.B., D'Asaro, E.A., 1994, J. Fluid Mech. 272, 255
Zahn, J.-P., 1991, A&AS 252, 179
Zahn, J.-P., 1992, A&AS 265, 115
Zirin, H., 1988, Astrophysics of the Sun, Cambridge University Press, Cambridge